FLOW CAMBRIDGE
UNIVERSITY PRESS

CRITICAL REVIEWS

A review of underwater shock and fluid–structure interactions

Helio Matos[1] , Mike Galuska[2], Carlos Javier[2], Shyamal Kishore[1], James LeBlanc[2] and Arun Shukla[1],*

[1]Dynamic Photo-Mechanics Lab, University of Rhode Island, Kingston, RI 02881, USA
[2]US Naval Undersea Warfare Center - Division Newport, Newport, RI 02841, USA
*Corresponding author. E-mail: shuklaa@uri.edu

Abstract

Underwater explosions are inherently complex and unique physical phenomena markedly distinct from those occurring above the surface. This distinctiveness is primarily attributed to the relatively incompressible nature of water, which fundamentally alters the propagation and impact of shock waves. The study of underwater explosions is paramount in applications such as underwater demolitions for construction and salvage operations. These applications require a comprehensive understanding in order to mitigate the disturbances' impact on marine structures and ecosystems. Studying underwater explosions and their mitigation encompasses various disciplines, including fluid mechanics, materials science and structural engineering. The work reviewed in this study contributes significantly to enhancing safety measures in marine structures by providing critical insights into the behaviour of structures under extreme conditions. This includes understanding the behaviour of gas bubbles formed by explosions, the transmission of shock waves through different media and the resultant forces exerted on structures submerged in water. Consequently, this review is meant to aid in designing robust and resilient marine systems capable of withstanding severe loading conditions caused by underwater explosions by providing key engineering considerations. The continuous evolution of this research area is essential for advancing maritime technology, ensuring the safety of undersea operations and protecting marine environments from the adverse effects of extreme subaqueous loadings.

Impact Statement

This manuscript analyses underwater shock and fluid–structure interactions, which are crucial for enhancing marine structure safety. It addresses the propagation of shock waves and bubble dynamics from underwater explosions, which is vital for designing resilient marine systems. The review integrates fluid mechanics, materials science and structural engineering to aid in constructing vessels and platforms, ensuring safety against extreme underwater disturbances and contributing to maritime technology and marine ecosystem protection. This work serves as a reference for understanding and mitigating underwater explosions.

1. Introduction

Underwater explosions (UNDEX) represent unique and complex phenomena that are significantly different from their above-surface counterparts due to the relatively incompressible nature of water

(Cole 1948; Shin 2004). The comprehension of UNDEX is crucial, not only for protecting maritime assets but also for various civilian applications, including but not limited to underwater demolitions, salvage operations and the study of marine life responses to subaqueous disturbances. Understanding the dynamics of an underwater explosion is vital for designing vessels and offshore structures, enabling engineers to predict and mitigate the potentially adverse effects of such events.

There are two primary mechanisms during UNDEX events: the initial shock wave and subsequent gas bubble. The propagation of shock waves and the behaviour of the gas bubbles necessitate in-depth analysis due to their ability to produce extreme loading on structures and marine life forms, making this topic a fundamental area of research within fluid dynamics and structural engineering. Regarding loading levels, approximately half of an explosion's total energy releases the shock wave, with the remainder feeding into the gas bubble's internal pressure, temperature and kinetic energy (Shin 2004). Both mechanisms must be considered to fully understand and predict UNDEX phenomena and their loading on nearby structures.

The behaviour of UNDEX events is highly variable, influenced by numerous parameters such as charge depth, weight, chemical composition, geometry, hydrostatic pressure, medium properties, proximity of boundaries and boundary mechanical properties. These factors will influence the shock wave's magnitude, duration and subsequent bubble dynamics, which include bubble volume, oscillation period and the properties of the bubble's gaseous contents. Notably, these parameters are often intertwined, creating a complex system to analyse. The intricate relationships among these factors can yield unpredictable outcomes, necessitating complex analytical and physical models to predict and mitigate the damage caused by UNDEX events.

Research on the physics of underwater explosion events dates back to the early 20th century, summarized by the seminal work of Cole, whose book *Underwater Explosions* (Cole 1948) is a cornerstone of the field. This volume encapsulates that era's extensive experimental and analytical efforts to understand UNDEX effects, providing the foundation for the equations and theories that describe shock waves and bubble dynamics resulting from underwater detonations. These early studies laid the groundwork for our current understanding and continue to influence how researchers analyse and prepare for the impacts of UNDEX on naval vessels and structures. This paper reviews the current understanding of UNDEX, especially regarding shockwave response, bubble dynamics and fluid–structure interactions.

2. Underwater blast

2.1. Shockwaves

2.1.1. Shock pressure

The shock wave generated by a UNDEX is a high-magnitude, short-duration compressive pressure wave that travels faster than the wave speed of the surrounding medium (Shin 2004). This phenomenon occurs instantaneously with the combustion and chemical decomposition of explosives, which produce gaseous byproducts at extremely high density and temperature (Cole 1948). The surrounding water is rapidly accelerated, causing a sharp, discontinuous increase in pressure, which then decays exponentially as the gaseous byproducts expand into a bubble. The shock wave radiates outward from the source of the explosion in a spherical wavefront, with its amplitude diminishing due to spherical spreading. As the expansion continues, the shock front velocity decelerates, eventually aligning with the water's acoustic speed (Shin 2004).

The characteristics of a UNDEX shock pressure wave, $P(t)$, can be captured by (2.1) (Swisdak 1978; Shin 2004). The amplitude, P_{max}, and decay constant, θ, can also be modelled using empirical (2.2) and (2.3). Although empirical relations, these equations mirror the dimensionless equations and solutions that describe strong shock waves in the air (Ramamurthi 2021), using explosive energy instead of weight and distance instead of hydrostatic pressure (since these parameters are proportional)

$$P(t) = P_{max}\, e^{-t/\theta}, \tag{2.1}$$

$$P_{\max} = K_P \left(\frac{W^{1/3}}{R} \right)^{\alpha_P}, \tag{2.2}$$

$$\theta = K_\theta W^{1/3} \left(\frac{W^{1/3}}{R} \right)^{\alpha_\theta}. \tag{2.3}$$

In these empirical equations, K_P, K_θ, α_P and α_θ are empirical constants that are specific to the explosive material, W is the mass of the explosive and R is the distance from the explosion to the point of interest. These equations illustrate the intensity of pressure near the explosion, highlighting that pressures can become exceedingly high as one approaches the explosion source. Similar equations can also be formulated to solve for energy and impulse with the fitting parameters for common explosive materials such as TNT (Swisdak 1978). The limitations of using these empirical equations lie in the parameters being tied to a specific explosive material and the range of the data used to determine the fitting parameters.

2.2. Gas bubble

2.2.1. Bubble dynamics overview

The gas bubbles from UNDEX events are comprised of explosive byproducts and rapidly phase-shifting water vapour engendered by the high temperatures of an exothermic reaction. Historically conceptualized as an oscillating gas globe or sphere in classical literature (Cole 1948), this bubble undergoes rapid radial expansion propelled by the exceedingly high pressure contained within. As it expands, the bubble's boundary is propelled outward spherically until it is curtailed by the external fluid pressure, eventually overcoming the internal pressure, causing the boundary velocity to decline and ultimately arrest at the bubble's maximum size.

Subsequently, the bubble enters a collapse phase, signified by the reversal of boundary velocity. This collapse releases a rarefaction wave, or an under-pressure wave, with sufficient force to potentially deform compliant structures. The collapse maintains a near-spherical shape in an unobstructed free-field setting. This infinite fluid domain is absent of any close structures, surfaces or boundaries to influence the flow induced by the bubble's oscillations. The bubble then contracts to a small but finite minimum size (determined by the volume of its condensable and non-condensable gases) before it grows outward again. When the bubble reaches its minimum size, a second shock wave, known as a bubble pulse, is released. Although less intense, this wave has a longer duration than the initial shock wave and results from the abrupt shift in boundary velocity at minimum size. Each successive expansion and collapse cycle diminishes the bubble's maximum radius and the strength of subsequent bubble pulses (Cole 1948; Shin 2004).

Free-field bubbles also exhibit an upward migration trend driven by buoyant forces from the pressure gradient along the bubble boundary. Larger bubbles experience more pressure change across this boundary, leading to a more pronounced ascension. Figure 1 offers a graphical representation of these general free-field bubble dynamics and the associated pressure changes, as shown by Shin (2004).

2.2.2. Free-field bubble empirical modelling

Cole (1948) discusses empirical formulas that delineate the peak pressure and duration of UNDEX shock waves and a free-field bubble's maximum radius and period across varying hydrostatic pressures and explosive charge masses. These formulas have found utility in characterizing various explosive materials (Swisdak 1978; Shin 2004) and accurately predicting their behaviour. Variations of these formulas, adapted to use imperial measurements, are presented in (2.4) and (2.5) (given in the SI-MKS unit system):

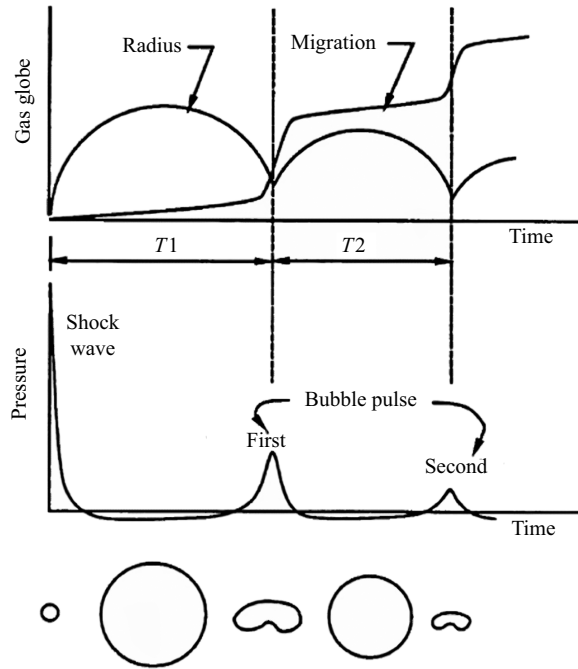$$R_{max} = K_R \left(\frac{W}{D + 10} \right)^{1/3}, \tag{2.4}$$

Figure 1. *Gas bubble growth, migration and bubble pulse (Shin 2004).*

$$T = K_T \frac{W^{1/3}}{(D + 10)^{5/6}}. \tag{2.5}$$

In these empirical equations, R_{max} signifies the bubble's maximum radius in metres, T is the period of the initial bubble oscillation in seconds, W is the explosive charge mass in kilograms, D represents the depth in metres and K_R and K_T are empirical coefficients that correlate with the specific type of explosive in use (in SI-MKS units, K_R is in $m^{4/3}/kg^{1/3}$ and K_T is in $s(m^{5/6}/kg^{1/3})$).

2.2.3. The energy of underwater shock and bubble
It is often necessary to model the shock and bubble pressure signatures in terms of their energy output. Measuring the energy output of an explosion event is critical because it helps quantify the loading to structures or systems impacted by the blast. For scientific research, such measurements can lead to a better understanding of explosive dynamics and developing predictive models. The energy terms associated with the total energy in an explosion event typically include the kinetic energy, the thermal energy released, the energy transmitted as shock waves through the medium and the potential energy associated with the gas bubble formation.

Previous work by Arons & Yennie (1948) looked into the energy partition during UNDEX events. These energy components include the irreversible energy flux contributing to the acoustic radiation as the shockwave travels away from the explosion source and the reversible after flow energy stored in the water due to fluid-particle movement during bubble formation and oscillations. The energy transferred to the surrounding medium (water) can be partitioned into various forms, but the work by Arons & Yennie (1948) focuses on the radiated energy and the energy related to the after flow process associated with the bubble dynamics post-explosion, which are the main components of the total energy in the system. The total radiated and reversible energy, E, for a spherical wave, can be found as a function of the pressure time history, P, and fluid properties, as shown in (2.6). Some energy terms are neglected in this equation due to their relatively small contribution to the total energy, including the kinetic energy imparted to the water and the change in internal energy in the mass of water as the shockwave
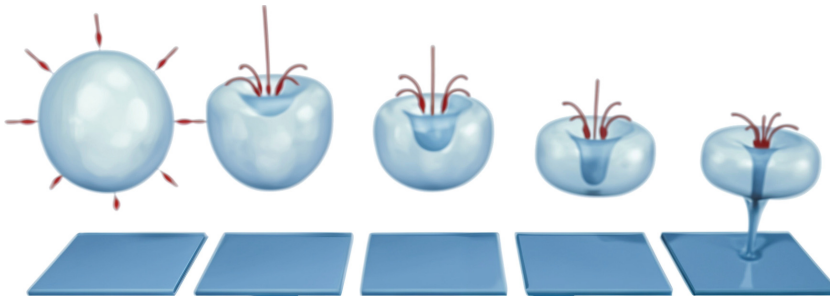
Figure 2. *Bubble collapse near a rigid barrier, resulting in jet formation.*

propagates. Furthermore, other energy components not explicitly considered in (2.6) but discussed in the work by Arons & Yennie (1948) include the total irreversible thermal, viscous and turbulent energy losses in water. These energy loss terms become critical for calculating the after flow energy after each subsequent bubble oscillation cycle

$$E = \frac{4\pi R^2}{\rho_o c_o} \int P^2 \, \mathrm{d}t + \frac{2\pi R}{\rho_o} I^2. \tag{2.6}$$

In this relationship, the first term represents radiated energy, and the second represents reversible energy. The R term is the radius from the explosive source to the spherical shock front, ρ_o the fluid density, c_o is the fluid's acoustic wave speed and I is the specific impulse of the pressure wave as defined by (2.7). The limits of integration for (2.6) and (2.7) are relative to when the shock pressure begins and ends

$$I = \int P \, \mathrm{d}t. \tag{2.7}$$

2.2.4. Near-field bubble dynamics

The interaction of UNDEX bubbles with nearby boundaries in their vicinity, termed 'near-field' interactions, carries the potential for severe structural loading. This is attributed to the formation of a re-entrant jet during the bubble's collapse in proximity to structures, which can have a destructive effect akin to a water hammer. This phenomenon occurs as a high-velocity jet of water thrusts into the bubble from the side opposite to the boundary, enabled by the high compliance of the gas within the bubble, which allows the jet to accelerate substantially, as illustrated in figure 2. The result is an intensely localized pressure that impacts a focused area of the structure (Javier *et al.* 2020*a*). These events are incredibly chaotic, and no reliable analytical models can be used for prediction purposes. Simulations of this phenomenon have been explored computationally, as illustrated in figure 3, and are discussed in more detail in § 5.

Collapses of underwater bubbles and cavities near structures have historically been shown to cause significant deformation and even corrosion. While 'near field' lacks a universally accepted definition, it typically refers to a scenario where a bubble's proximity to a boundary – such as a structure or free surface – is close enough to cause consequential fluid–structure interactions or influence the bubble dynamics. In these near-field cases, the structure can inhibit bubble expansion by constraining fluid motion on one side, leading to an asymmetric bubble growth cycle and, potentially, to the formation of a bubble jet. A range of factors influences the trajectory of this jet: the distance between the explosive charge and the structure, known as the standoff distance; the effects of buoyant forces; the structure's compliance, shape and boundary conditions; and the presence and positioning of additional structural elements or free surfaces (Javier *et al.* 2020*a*; Leger *et al.* 2023).
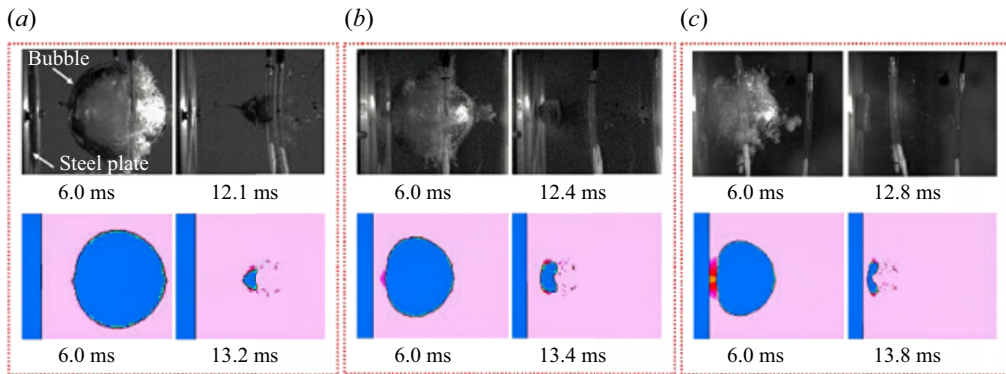
Figure 3. *Experimental and simulated maximum and minimum bubble volumes for standoff distances of (a) γ = 1.5, (b) γ = 1.0 and (c) γ = 0.75 (Javier et al. 2020a).*

2.2.5. Near-field bubble jetting

The study of gas bubble dynamics traces back to Rayleigh's analytical model of a spherical bubble collapsing in a free-field environment, established in 1917 (Rayleigh 1917). Research on near-field rigid boundary jetting expanded significantly after Konfeld & Suvorov's (1944) proposition that bubble jetting was the principal cause of cavitation damage. Benjamin and Ellis's experiments supported this hypothesis of a liquid jet forming during bubble collapse (Benjamin & Ellis 1966), which produced high-speed photographic evidence of bubbles generated by electrical sparks. They also suggested applying the analytical Kelvin impulse concept to evaluate the fluid momentum of an asymmetrical cavitation bubble. An experimental investigation by Naudé & Ellis (1960) honed in on the loads caused by bubble jetting and the interaction of the bubble boundary, employing photoelastic materials to visualize the stress conditions induced on the boundary.

Plesset & Chapman (1970) then advanced a numerical method predicated on a Rayleigh bubble to forecast these loads and utilized the water hammer principle to estimate the likely jet velocities and pressures. Lauterborn & Bolle (1975) validated this computational approach by experimentally determining jet tip velocities through high-speed photography.

Pioneering studies of gas bubbles in proximity to other types of boundaries, including free surfaces and compliant boundaries, were conducted by Gibson (1968). His experiments analysed the differences in jet behaviour and bubble–structure interactions at various explosive standoff distances, demonstrating that greater standoff distances diminish the potential for jetting and interaction with the structure.

The implications of standoff distances on bubble jetting were further examined in a small-scale UNDEX study by Javier *et al.* (2020a). Their research delved into the pressures experienced by specimens due to bubble jetting against the surface of a rigid boundary. Both experimental approaches and numerical simulations were employed to capture the phenomenon. High-speed photography was utilized to record the bubble jetting, and the results were compared with numerical solutions for three dimensionless standoffs. The findings are shown in figure 3, which illustrates that reduced standoff distances (represented by the dimensionless parameter $\gamma = \text{Standoff}/R_{max}$) lead to more pronounced jetting towards the rigid boundary.

2.2.6. Damage of shock waves and explosions

Underwater explosion shock waves are recognized for their potential to damage structures, which is relevant in far-field and near-field scenarios. Kennard (1944) conducted a seminal analytical investigation into the shock loading of air-backed plates and diaphragms of infinite size. His predictions encompassed damage assessment, surface cavitation and the impact of baffles on structural distortion. The studies by Taylor (1963) and Friedlander (1941) delved into the reflected pressures and structural reactions of plates with varying degrees of rigidity and compliance when subjected to shock waves.

It has been established that vaporous surface cavities can develop on certain structures due to underwater shock, particularly in situations characterized by low hydrostatic pressure and high specimen velocities (Pavlov & Galiev 1977). These surface cavities engage with the structure, exacerbating structural deformation. Galiev conducted parallel experimental (Galiev 1979) and theoretical (Galiev 1987) inquiries, positing that the impulse imparted by a shock wave is more critical than its magnitude in determining the resulting deformation. His numerical analyses forecasted the initiation of cavitation stemming from shock wave reflections. In a subsequent study, Galiev examined the phenomena of liquid jets striking submerged targets (Galiev 1995), predicting the genesis of a cavitation zone akin to that identified by Friedlander (Friedlander 1941). He noted this zone's dependency on the wavelength of the incident pulse, which could amplify peak deflection by a factor of two to three. Following this line of inquiry, experimental work was expanded to encompass a range of elastic-plastic plate materials and configurations, such as circular and rectangular plates (Galiev 1997).

2.2.7. Damage from near-field gas bubbles

Ramajeyathilagam *et al.* undertook a series of UNDEX shock loading experiments and computational damage assessments for various structures, including thin rectangular plates (Ramajeyathilagam *et al.* 2000; Ramajeyathilagam & Vendham 2004), cylindrical plates (Ramajeyathilagam *et al.* 2001) and panels with differing curvatures (Ramajeyathilagam & Vendham 2003). These tests were likely influenced by bubble effect loading due to the substantial explosive charges and the relatively close detonation distances. The researchers analysed postmortem specimens to gauge plastic deformation and rupture. They compared their findings with a theoretical rupture strain model integrating effective plastic strain (Ramajeyathilagam & Vendham 2004) to enhance simulation rupture prediction. The failure modes identified in these panels, depicted in figure 4, predominantly featured edge tearing and central petalling. The research emphasized the criticality of incorporating strain rate-dependent material models in UNDEX experimental simulations. Suresh replicated these experiments using a coupled fluid–structure interaction (FSI) model in LS-DYNA, addressing both non-rupture (Suresh & Ramajeyathilagam 2020) and rupture scenarios (Suresh & Ramajeyathilagam 2021). Riley *et al.* (2010) experimented with air-backed circular and square thin plates subjected to near-contact explosions. These scenarios were modelled using LS-DYNA to compare the central ruptures with actual test results, as shown qualitatively in figure 5, without accounting for bubble effects. Hung *et al.* (2005) employed experimental pressure data within a finite element analysis framework to predict the response behaviours of specimens.

The collapse of UNDEX bubbles generates additional shock waves, a phenomenon studied by Arons *et al.* (1948), Arons (1948). These secondary shock emissions, while less intense in peak magnitude than the initial wave, persist longer. The researchers proposed using point impulse integrations of pressure–time plots to evaluate the potential damage from each shock wave. Their findings confirmed that UNDEX gas bubbles oscillate, dissipating their energy gradually. Chapman's study (1985) provided insights into predicting the peak and duration of these pulses following multiple collapses, also considering the effects of buoyancy, hydrostatic pressure and bubble migration on this dynamics. These studies illustrate that the impulse magnitude of the bubble collapse is significant and should be considered during near-field UNDEX problems.

2.2.8. Challenges and limitations

The insights gained from most studies that analyse small, spark or laser-induced gas bubbles under low hydrostatic pressure conditions do not fully translate to understanding the damage potential from UNDEX events. The shock wave generated by an explosive event poses a risk of structural damage and can inhibit bubble growth. Underwater explosion bubbles are typically larger, facing more intense internal pressures and temperatures and experiencing greater pressure gradients, which lead to stronger buoyancy forces. Whereas small cavitation bubbles may only result in pitting on near-field materials, these effects might not be consistent when scaled up to larger structures or when other forms of damage are considered. Moreover, the potential energy contained in larger UNDEX bubbles can render even
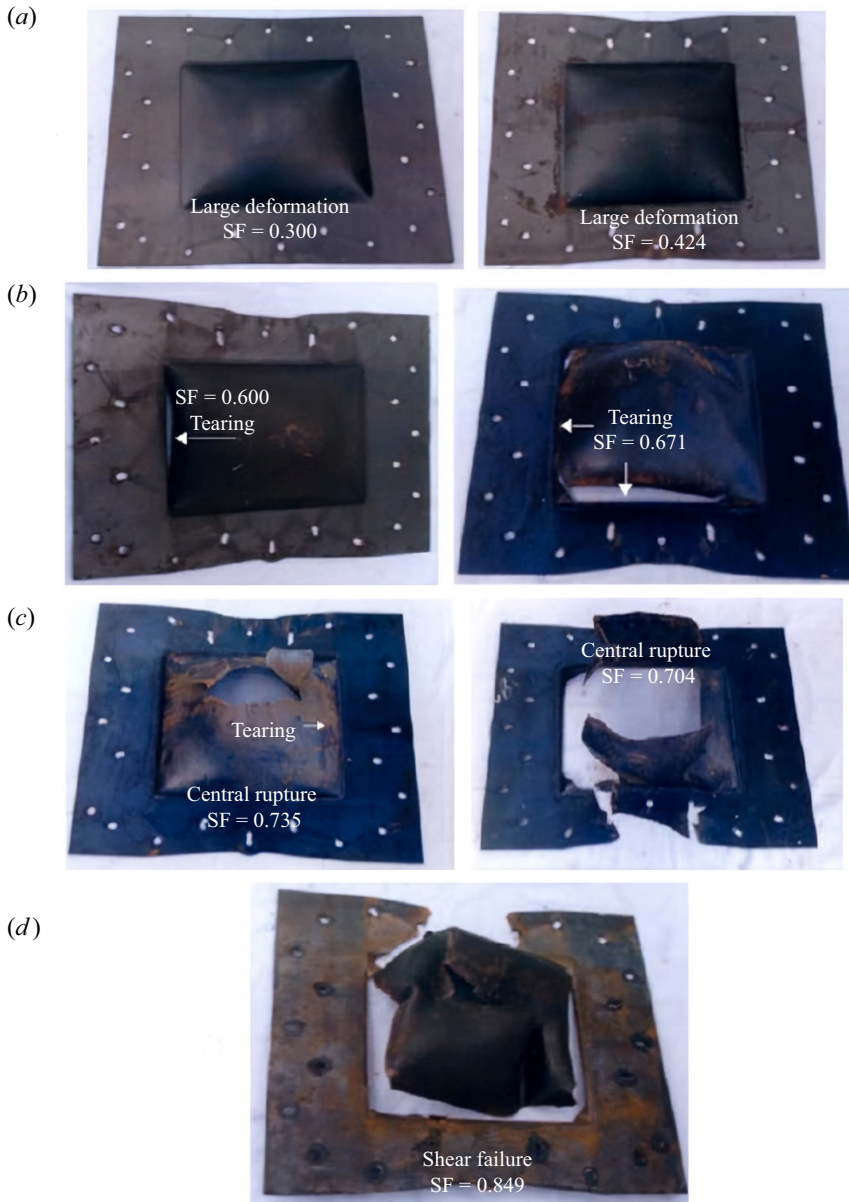
(*a*)

(*b*)

(*c*)

(*d*)

Figure 4. *Failure modes of mild steel plates: (a) large deformation (mode I), (b) tensile tearing (mode II), (c) central rupture (mode III) and (d) combined shear failure and tensile tearing (modes II–III) (Ramajeyathilagam & Vendham 2004).*

thick metal specimens like aluminium or steel relatively compliant in the face of the extreme velocities and pressures generated by bubble jetting.

3. Damage mitigation

Emerging technologies and solutions for underwater blast mitigation and structural protection during UNDEX events are crucial in enhancing the safety and durability of marine structures and equipment. The complexity of UNDEX scenarios, characterized by intense shock waves and unique FSIs, requires
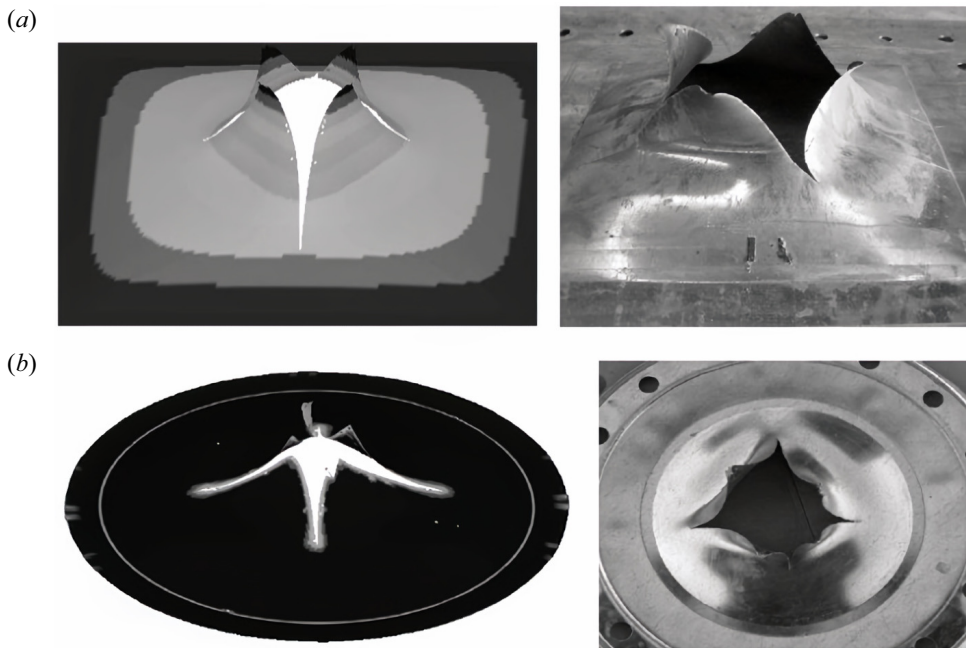
(a)

(b)

Figure 5. *Final petal formation in numerical and experimental contact charges for (a) 350WT steel and (b) A653 steel (Riley et al. 2010).*

innovative approaches. This discussion outlines several key emerging technologies and solutions in this field. The approaches discussed here are predominantly passive techniques designed to absorb, disrupt and reduce the effect of the shock/blast waves.

3.1. Polymer-based mitigation solutions

Polymer-based composites are increasingly employed in marine industries for their superior blast mitigation capabilities (Wanchoo *et al.* 2021). These composites are generally found in three forms: external polymer skins or coatings, internal sandwich composites or integrated within the base material of polymer-modified structures. Polymer coatings, which can be applied to interior and exterior surfaces, play a significant role in shielding against blast loads, although their effectiveness can vary. Sandwich composites are particularly notable for their design, which enables them to achieve higher shear and bending stiffness-to-weight ratios, greatly enhancing their ability to absorb impacts and dissipate energy from intense blasts (Wanchoo *et al.* 2021). Lastly, in polymer-modified structures, often seen in fibre-reinforced composites, the matrix is typically enhanced with an elastomer compound, adding to the material's resilience and blast mitigation properties (Wanchoo *et al.* 2023).

3.1.1. Polymer-coated plates

Polyurea for coating applications is favoured for its rapid curing, chemical resistance, fire, corrosion resistance and high stiffness under loading rates (Roland *et al.* 2007). In air blast scenarios, it has successfully reduced deformation in steel and composite plates (Yi *et al.* 2006; Tekalur *et al.* 2008; Mohotti *et al.* 2021). LeBlanc and others have explored damage mitigation in composite structures, showing that coating thickness and placement significantly influence underwater blast resistance. For instance, curved plates with thicker back-face coatings displayed reduced deformations
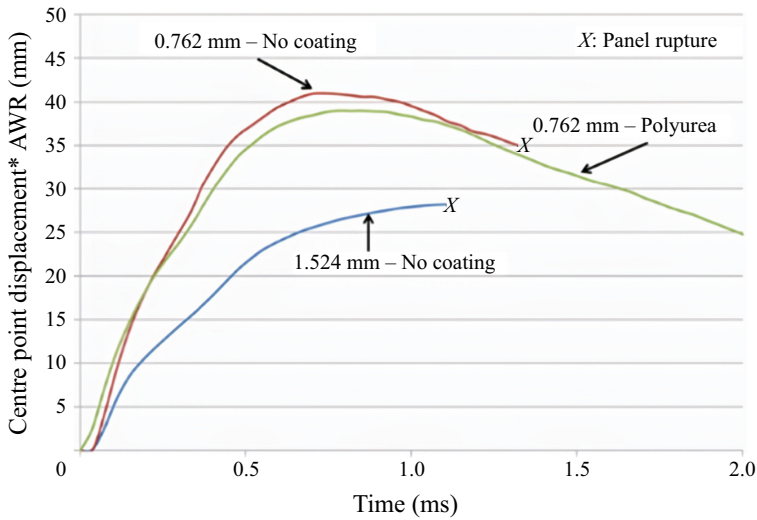
Figure 6. *Centre point out-of-plane displacements of composite plates, adjusted by areal weight (AWR), with and without polyurea coating (LeBlanc et al. 2016).*

(Leblanc *et al.* 2013; Leblanc & Shukla 2015). Li *et al.* found that front-face coatings on isotropic aluminium plates were more effective than back-face coatings in far-field explosions (Li *et al.* 2019), while LeBlanc *et al.* observed that air-backed flat composite plates coated on the back face with polyurea resisted rupture under similar conditions, as illustrated in figure 6 (LeBlanc *et al.* 2016). In contrast, Dai's study on metal plates suggested that front-face polyurea coatings offer better mitigation, highlighting the role of bond strength between the polyurea and the substrate (Dai *et al.* 2018). Liu *et al.* observed that steel plates with front-face coatings had lower final deformation than those with back-face coatings (Liu *et al.* 2022b), illustrated in figure 7, and further research showed that dual-faced polyurea applications could be more effective than single-sided ones, illustrated in figure 8 (Liu *et al.* 2022a).

3.1.2. Polymer-coated cylinders

Similar investigations have been conducted on hollow cylinders, with studies examining the effects of rubber and polyurea coatings under UNDEX conditions. Kwon's numerical analysis on aluminium and steel cylinders with rubber coatings revealed that, while these coatings can trap shockwave energy, increasing the rubber's shear modulus and thickness could improve energy mitigation (Kwon *et al.* 1994). Gauch's experiments on carbon fibre/epoxy hollow cylinders coated with polyurea showed significant damage reduction, particularly with thicker coatings, as illustrated in figure 9 (Gauch *et al.* 2018). Nayak developed a machine learning algorithm to analyse the behaviour of polyurea-coated composite cylinders, concluding that such coatings' protective effects largely depend on their thickness (Nayak *et al.* 2022).

These studies collectively indicate that polymer coatings, especially polyurea, are a promising solution for mitigating damage from UNDEX. The effectiveness of these coatings, however, varies based on factors like coating thickness, placement and the specific material properties of a front-face application. Contrary to some previous findings, the data also indicate that a dual-faced polyurea application has a superior mitigative impact than coating solely on the front or the back face. These results illustrated that polymer coating systems may be an effective solution to mitigate damage from UNDEX. However, the optimization of the coating locations depends on the structural performance and the shock loading condition.
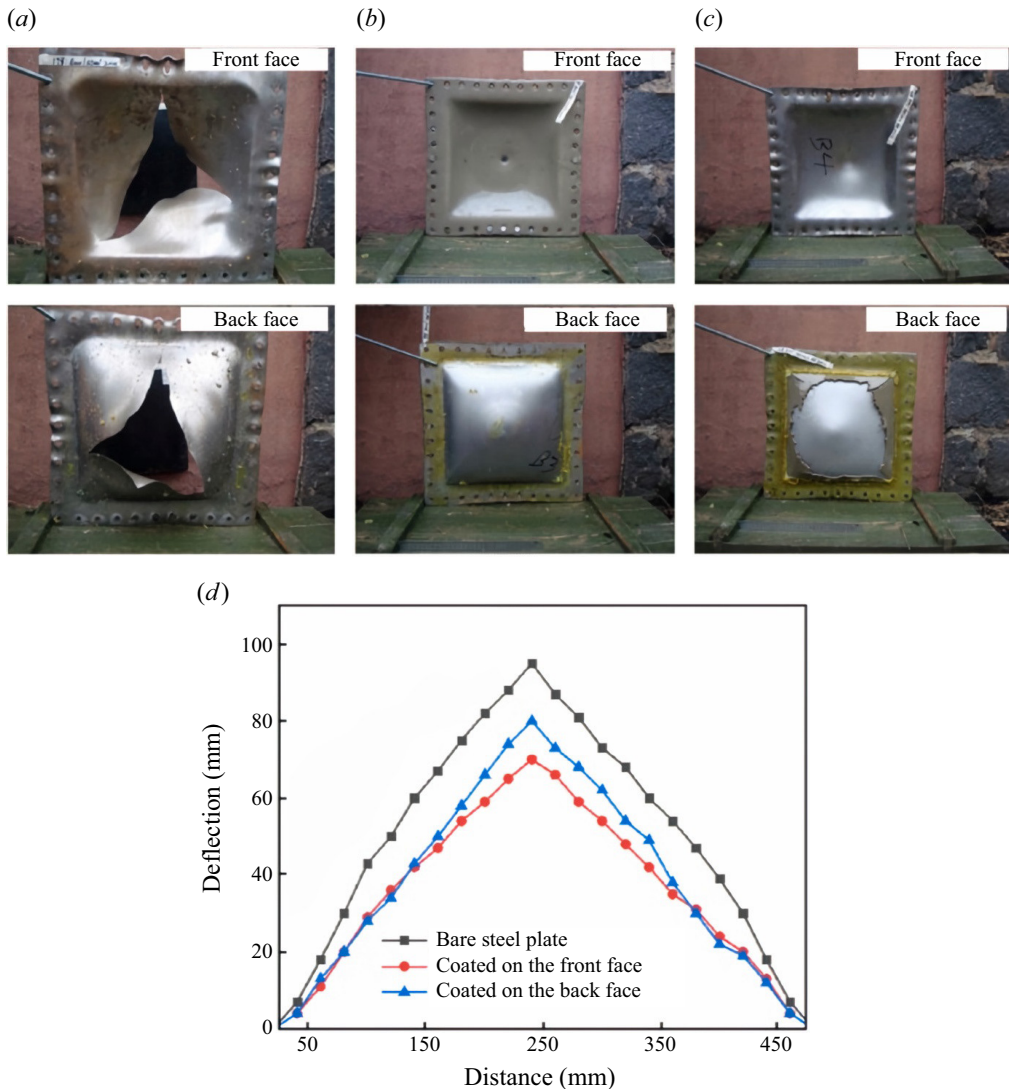
Figure 7. *Postmortem images for three polyurea coating methods on steel plates (D = 8 mm): (a) the bare steel plate; (b) front-face polyurea coating (4 mm); (c) back-face polyurea coating (4 mm); (d) deformation profiles of the steel plates (Liu et al. 2022b).*

3.1.3. Sandwich composites

As previously mentioned, sandwich composites are increasingly recognized for their effectiveness in mitigating underwater shock, particularly during UNDEX events. These composites, comprising high-strength face sheets and a lightweight core (such as polymeric foams or honeycomb structures), offer a unique combination of strength and energy absorption. The core material is critical in dissipating the energy from shock waves, thereby reducing peak stresses and potential damage (Wanchoo et al. 2021). Much like the differences with coating systems, no universal solution would be ideal for dissipating every type of UNDEX loading. The loading case's specifics must be considered when designing a sandwich structure. There is also much ongoing work on novel core designs, such as auxetic and lattice structures for shock mitigation due to technological advancements in manufacturing (Wanchoo et al. 2021).
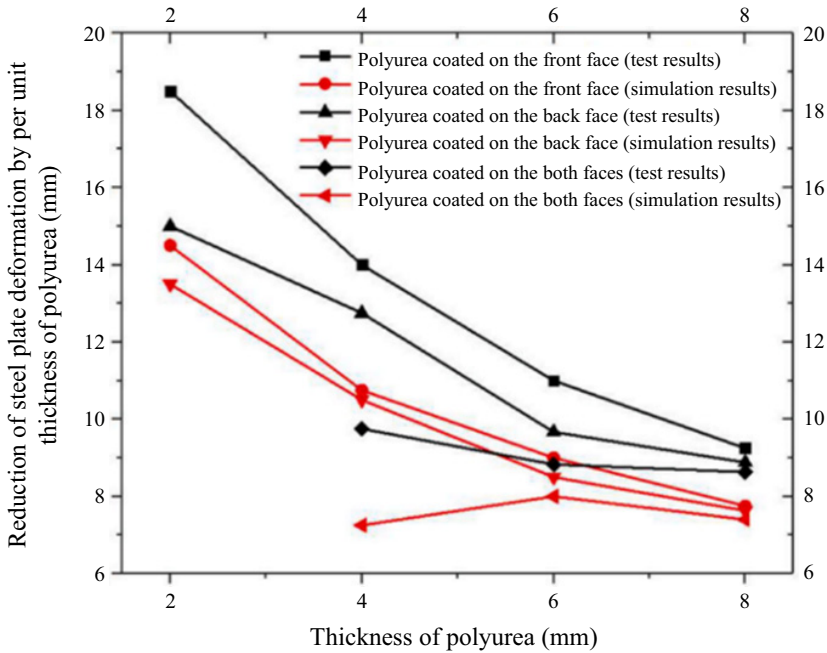
Figure 8. *Maximum deformation as a function of polyurea coat thickness for plates with various coating methods (Liu et al. 2022a).*
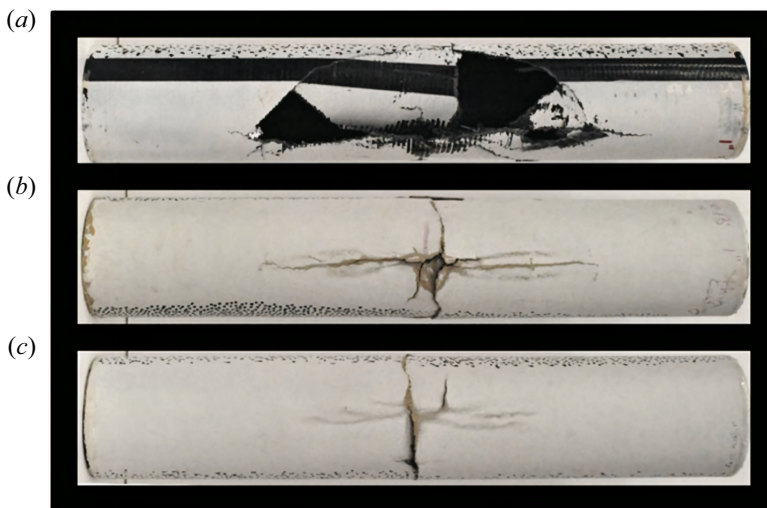

Figure 9. *Exterior view of cylinder damage – 2.54 cm charge standoff, (a) uncoated, (b) thin coating (2.34 mm thickness), (c) thick coating (3.04 mm thickness) (Gauch et al. 2018).*

3.1.4. Polymer-modified structures

Polymer-modified structures offer enhanced mitigation against blast loads due to their improved toughness and energy absorption properties. The modifications in the matrix resin, including liquid rubbers and pre-formed rubber particles, enhance the overall response of the composite structure to dynamic loadings such as UNDEX loadings. These changes improve the structural damping and energy dissipation under below-failure shock loadings and exhibit limited crack growth under high-intensity shock

conditions. Studies have shown that these viscoelastic materials become more dissipative with increasing loading frequency, although they may become hard and non-dissipative at very high frequencies (Wanchoo *et al.* 2023). While these modifications significantly increase the impact resistance and shock absorption capabilities, a notable limitation is the base resin's reduction in modulus and strength due to the inclusion of these modifiers (Wanchoo *et al.* 2023).

3.2. Emerging technologies and other solutions

Several other types of systems can lead to blast and shock mitigation. A recent review by Wanchoo *et al.* (2021) discusses many of these techniques for UNDEX events. Some of the techniques (besides the polymer-based solutions already presented) are discussed in the following subsections.

3.2.1. Impedance mismatching

Impedance mismatching is a technique that leverages the difference in acoustic impedance between different materials to enhance stress wave reflection. By strategically choosing materials for the protective layer that significantly differ in impedance from the underlying structure, the stress waves resulting from an explosion may be effectively reflected away. This mismatch minimizes the transmission of shock wave energy into the protected structure, thereby reducing the potential damage. It is particularly effective when the shock wave's energy can be redirected rather than absorbed. Hence, this mitigation approach has the opposite effect of polymer coating.

3.2.2. Protective cladding

Protective or sacrificial cladding involves the use of materials that can absorb and dissipate the energy of the blast wave, thus protecting the underlying structure. This technique reduces the stress transferred to the structure and increases the loading duration, spreading the impact. The cladding materials often undergo plastic deformation or destruction, sacrificing themselves to protect the primary structure (Wanchoo *et al.* 2024). Due to the cladding destruction, this mitigation approach is exceptionally effective but may be limited to a single use, unlike polymer coatings, which may be designed for multi-use. Materials used for cladding are chosen for their energy absorption capabilities and could include advanced composites, foams or specialized alloys.

3.2.3. Geometrical and structural features

Geometrical arrangements in design play a crucial role in deflecting or redirecting blast waves away from critical areas of a structure. By strategically designing the shape and orientation of structures, the impact of a blast wave can be mitigated. This might involve curved surfaces (Leger *et al.* 2023), angled panels or specific structural contours that channel the energy of the blast wave in a less harmful direction. This approach is advantageous in large-scale structures where direct absorption of blast energy is impractical. Other new areas that include this type of energy mitigation include metamaterials and metastructures with substructural-scale features incorporated for energy mitigation purposes (He & Fan 2021).

3.2.4. Blast-wave disrupters

Blast-wave disrupters are structures or materials placed between the source of the blast and the protected structure. These disrupters act as barriers or baffles, breaking up and diffusing the energy of the blast wave. They can be specially designed structures or materials that fragment or deform under blast pressure, disrupting the blast wave's continuity and intensity. The effectiveness of these disrupters depends on their material properties, design and placement relative to the protected structure and the anticipated blast source (Wanchoo *et al.* 2021).

3.3. Addressing fluid–structure interactions

Understanding and addressing the complex interactions in underwater environments is vital. The higher density of water compared with air results in more momentum carried by the post-shock particle movement. Factors like shock wave reflections from boundaries such as the sea floor, cavitation zones and the creation of high-pressure water jets due to gas bubble collapses are integral to designing effective mitigation strategies (Wanchoo *et al.* 2021). The following are mitigation discussions for the bubble dynamics phenomena discussed in §§ 2.2.4 through 2.2.7. The emphasis of this discussion is on bubble jetting due to its high destructive potential.

3.3.1. Mitigating of bubble jetting

Gibson's study (1968) delved into the nuances of jetting behaviours associated with different boundary conditions, making significant observations. Particularly noteworthy were the jetting patterns that deviated from free surfaces when subjected to minor buoyant forces – typically observed in smaller bubbles with brief collapse durations. Moreover, in scenarios involving flexible boundaries, small standoff distances led to the absence of jetting, while increased standoff distances resulted in jetting that veered away from the boundary. This behaviour highlights the potential of flexible boundaries to significantly reduce the risk of structural damage caused by the collapse of near-field bubbles.

Gibson suggested the use of flexible coatings on rigid surfaces to create a boundary that would be more compliant. An increase in compliance can neutralize or even reverse the direction of jetting. Gibson & Blake (1982) expanded upon this idea by suggesting amendments to the Kelvin impulse formulation, aiming to predict the jetting direction when dealing with elastic boundaries conceptualized as a spring–mass damper system. Their research compared the jetting behaviours of plain flexible rubber sheets against rubber-coated rigid boundaries. The findings revealed that while the flexible and coated surfaces exhibited repulsive jetting, the stiffer rubber options displayed annular jetting. This latter type of jetting led to the bubble splitting and subsequent formation of linear jets shooting in opposite directions post-collapse.

The culmination of their findings and methodologies can be found in their 1987 publication (Blake & Gibson 1987). Visual aids in their work offer a clearer understanding of these concepts: figure 10 outlines a parameter space that correlates the impact of the dimensionless standoff, γ, with the buoyancy parameter, δ, on the direction of bubble jetting against rigid boundaries. Furthermore, figure 11 illustrates the varied jetting behaviours when interacting with an array of compliant surfaces, demonstrating both annular jetting, shown in (*b*,*c*), and repulsive jetting, depicted in (*a–d*).

Shima *et al.* (1988) extended the exploration of the bubble dynamics by examining composite specimens, specifically by adding foam and a viscoelastic layer to brass plates. Their investigations indicated that the phenomena of attractive and repulsive jetting are influenced by the standoff distance and the foam rubber layer's thickness. In parallel, Duncan *et al.* (1996) developed a numerical model that simulates bubble dynamics and the energy transfer to elastic coatings. His model showed good concordance with the experimental results of Gibson & Blake (1982) as well as with Shima *et al.* (1988).

Brujan *et al.* (2001) experimentally delved into the effects of elastic moduli on jetting behaviours, uncovering that attractive jetting occurred at very close standoffs. They also identified a substantial range where bubble splitting was prevalent and, beyond that, a range indicative of repulsive jetting. Significantly, they observed that the velocity of jets in bubble-splitting scenarios was notably higher than that in cases of attractive jetting, which implies a potential for greater damage compared with rigid boundaries and highlights possible adverse outcomes from using flexible coatings.

4. Long-term structural shock performance

Fibre-reinforced composite structures are increasingly used in marine environments due to their favourable strength-to-weight ratio and low radar and noise signatures. However, these structural systems are also susceptible to seawater degradation after prolonged exposure to seawater (Davies 2016).
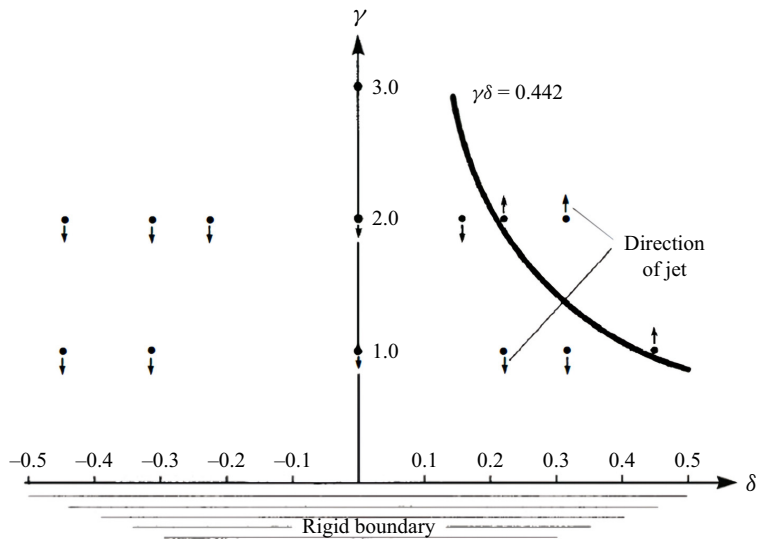
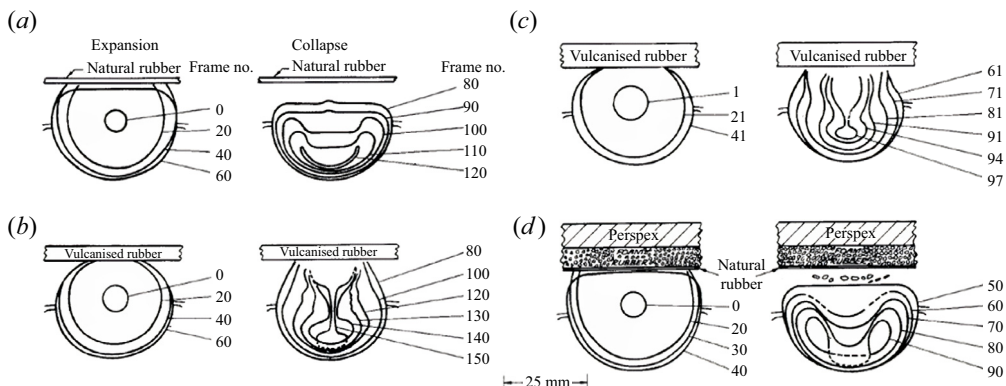**Figure 10.** *The $\gamma-\delta$ parameter space for buoyant vapour bubbles (Gibson & Blake 1982).*

Figure 11. *Examples of the interaction of pulsating bubbles with various deformable surfaces (Gibson & Blake 1982).*

During this prolonged exposure, materials' mechanical and blast mitigation properties will degrade due to plasticization and the reduction of mechanical properties. Another key degradation mechanism for marine environments is ultraviolet (UV) radiation and combined UV and seawater degradation. Emerging solutions include the application of external polymer coatings on undersea structures to reduce environmental degradation and enhance blast mitigation capabilities (Wanchoo *et al.* 2021).

4.1. Seawater degradation of composites

The work by Kumar highlights how exposure to saline water and UV radiation negatively impacts the matrix-dominated properties, such as transverse modulus and strength, of carbon fibre/epoxy materials (Kumar *et al.* 2002). Complementing this, Rice developed a method to simulate long-term water absorption in composites, revealing an accelerated water diffusion rate under hydrostatic pressure, primarily in the voids between fibres and the matrix (activation energy calculation; Pollard *et al.* 1989;
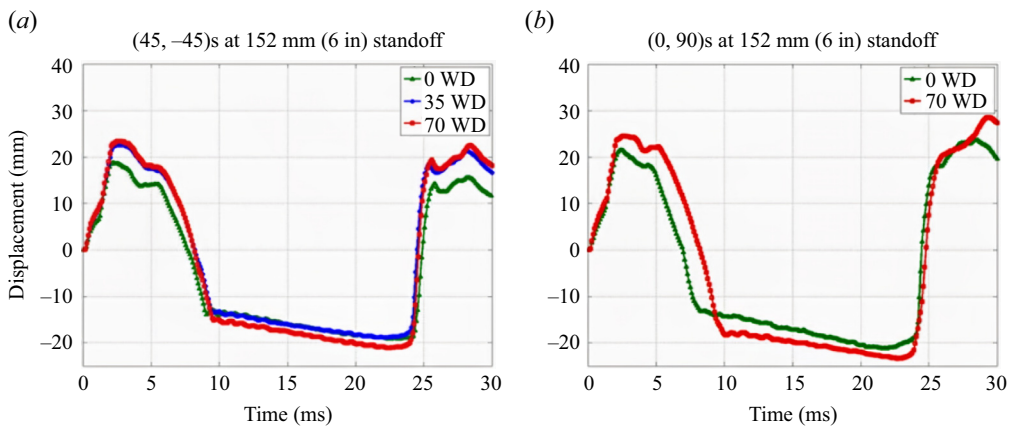
(a)
(45, −45)s at 152 mm (6 in) standoff

(b)
(0, 90)s at 152 mm (6 in) standoff

Figure 12. *Centre point out-of-plane displacements for (a) (±45)s fibre layup composites in comparison with unexposed controls (b) (0, 90)s layup composites compared with unexposed controls. WD, weathering days.*

Humeau & Davies 2015; Chen *et al.* 2017). Building on these insights, Shillings conducted experiments by immersing carbon fibre/epoxy composite plates in saline water to simulate extended exposure. This study found that plates exposed to saline water showed increased out-of-plane displacements when subjected to an in-air blast compared with their non-exposed counterparts (Shillings *et al.* 2017). This finding is contrasted by Fontaine's research, which tested composites undersea floor pressure conditions and concluded that such high-pressure exposure did not significantly alter the blast response of the materials (Fontaine *et al.* 2021). Collectively, these studies illustrate the nuanced ways in which environmental conditions impact composite materials.

Further extending the understanding of environmental effects, Javier investigated the impact of UV radiation on composite plates. This study noted a reduction in mass and changes in mechanical properties post-UV exposure. E-glass/vinyl ester plates exhibited decreased failure stress and strain, whereas carbon fibre/epoxy plates showed improved properties after UV exposure. When these plates were exposed to an in-air blast, the UV-exposed ones demonstrated less centre point out-of-plane displacement, suggesting a stiffening in mechanical properties due to UV exposure (Javier *et al.* 2019). This research provides a comprehensive view of how different environmental factors distinctly affect the durability and performance of fibre-reinforced composites.

4.2. Shock response after prolonged environmental exposure

The resilience of composite plates and cylinders to UNDEX detonations after prolonged exposure to marine environments has been a recent research focus. Matos *et al.* (2018) studied submerging carbon fibre/epoxy plates in saline water for periods equivalent to 10 and 20 years, based on the Arrhenius relationship (Chaudhary *et al.* 2023) and average ocean water temperatures. These plates were then subjected to near-field UNDEX blasts. The results, captured using high-speed cameras and three-dimensional digital image correlation, revealed greater displacement in saline-exposed plates than controls, as shown in figure 12. The study noted that saline-exposed plates showed more damage, with (±45)s layup plates demonstrating significant decreases in residual strength related to shear-dominated mechanisms.

Complementing this, Javier investigated the effects of water-backing and fluid hydrostatic pressure on UNDEX-affected plates (Javier, Leblanc & Shukla 2020b). Plates immersed in saline water and tested under different hydrostatic pressures showed that at 0 MPa, saline-exposed plates experienced increased displacement, but at 3.45 MPa, displacement changes were negligible, indicating that at
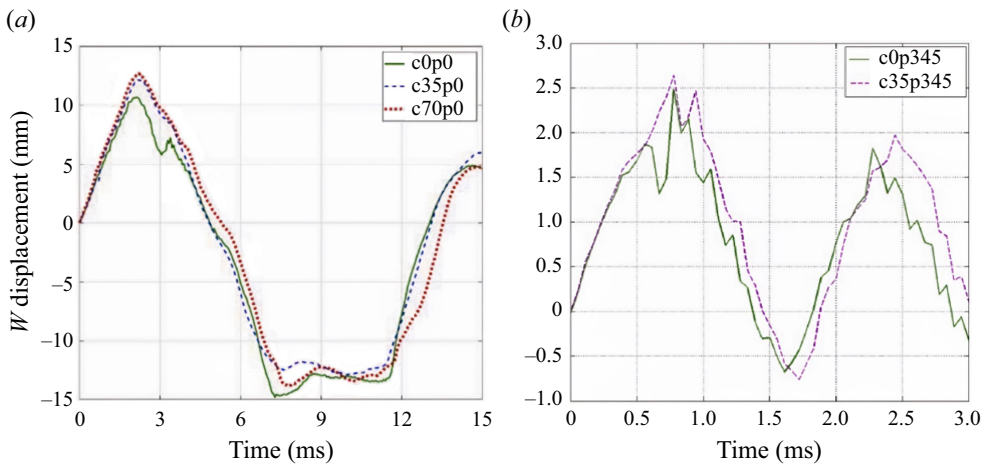
Figure 13. *Out-of-plane displacements of water-backed plates (a) 0 MPa gage pressure, saline-exposed composites vs. control (b) 3.45 MPa gage pressure, saline-exposed composites vs. control.*
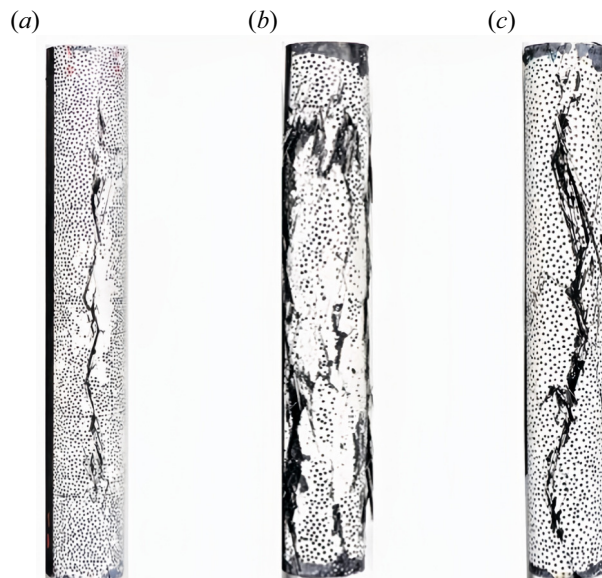

Figure 14. *Postmortem images for UNDEX blast-initiated implosion of composite cylinders with (a) no saline water exposure, (b) 35 days of laboratory exposure to saline water (equivalent to 10 years of natural water ingress) and (c) 70 days of laboratory exposure to saline water (equivalent to 20 years of natural water ingress).*

certain pressures, the UNDEX response may align with unexposed plates, as illustrated in figure 13. Additionally, the response of composite cylinders to saline water exposure under UNDEX blast loads was examined (Javier *et al.* 2018). Cylinders immersed in saline water and subjected to blasts in a pressure vessel showed significant damage, particularly for those immersed for 35 days compared with 70 days. This finding suggests a slight change in mechanical properties upon saturation, yet cylinders with prolonged saline exposure still exhibited more damage than unexposed ones, as depicted in figure 14. These studies collectively provide insights into the effects of saline water exposure on the structural integrity of composite materials in extreme loading conditions.

4.3. Exposure of polyurea to marine environments

Coating systems are not only used to prevent blast mitigation but also to slow down underwater systems' degradation (Chaudhary *et al.* 2024). However, the polymer coating itself will also undergo its own degradation. Polyurea, for instance, will deteriorate under marine conditions, including exposure to saline water and UV radiation, potentially impacting its protective capabilities. Mforsoh's study investigated how these factors affect polyurea (Neba Mforsoh *et al.* 2020). The research involved immersing polyurea samples in saline baths at various temperatures to understand the effect of temperature on water ingress. Additionally, samples were subjected to UV radiation and a combination of UV and saline exposure. Mechanical properties were evaluated using quasi-static and dynamic compression tests. The results showed an increase in elastic modulus and strain energy after UV radiation exposure, with dynamic tests indicating an increase in strain energy following UV exposure but a decrease after saline immersion. Interestingly, samples exposed to saline water and UV radiation exhibited significant differences in stress and strain energy compared with those subjected to a single element.

Complementing this, Chenwi focused on the degradation at the interface between polyurea and substrates post-saline immersion (Chenwi *et al.* 2022). After prolonged saline exposure, this study examined the peel strength changes between polyurea coatings and Monel 400, a nickel–copper alloy. Coated with polyurea, the specimens were bathed in saline water at 70 °C for 2 to 8 weeks to accelerate aging. Peel strength measurements indicated a notable decrease in bonding strength; an 83 % reduction in peel strength at the polyurea-Monel 400 interface was observed after eight weeks. This research highlights the deterioration of polyurea's mechanical properties due to saline water exposure and the weakened bonding at the interface with its substrates.

5. Modelling of fluid–structure interactions

5.1. Analytical modelling

This section explores analytical modelling techniques used to characterize FSI phenomena during underwater shockwaves. Such phenomena are particularly critical underwater due to the significantly lower acoustic impedance mismatch between solids in water than in air. Analytical models offer physics-based understanding, helping to develop new scaling laws, guide parametric study designs, and contribute to reducing computational costs. Despite these advantages, analytical modelling remains challenging and has not progressed as far as computational efforts, especially for near-field shock events.

5.1.1. Analytical background
Early explorations by Cole (1948), Ezra (1973), Keil (1961) and Kennard (1944) shed light on the interactions between shock waves and plane plates, complemented by Chertock's equations (Chertock 1953) on how water alters vibration modes and frequencies in submerged solids. Taylor's work (Taylor 1963), a milestone in FSI modelling, introduced a method to calculate pressure pulse reflection and plate deflection. Building on this, Temperley (1950) investigated cavitation during pressure pulse interactions, and Xue & Hutchinson (2004) provided a comparative analysis of FSI in different plate backing scenarios. The work of McMeeking *et al.* (2008) expanded Taylor's model, focusing on varied sandwich core topologies and cavitation FSI, followed by several studies (Ramajeyathilagam & Vendham 2004; Deshpande & Fleck 2005; Espinosa *et al.* 2006; Rajendran *et al.* 2006; Teich & Gebbeken 2013) delving into more complex loadings on air-backed plates. Liu & Young (2008) refined Taylor's model for water-backed plates within the acoustic range. Despite these advancements, there remains a notable gap in understanding dynamic plate bending response and the effects of near-field fluid-particle velocities post-pressure wave impact, a gap highlighted by Arons & Yennie (1948) and Keil (1961). Recent models, including those by Wang *et al.* (2013), Junger & Feit (1986 and Kim (2010) have yet to fully address these factors, particularly in the context of impulse loads, underscoring the need for further research in this area.

Table 1. *Summary of analytical shock interaction models.*

Model description	Fluid-particle velocity, v_k	Continuity	Motion of plate element
Single degree of freedom air backed	$\dfrac{p_k}{\rho_w c}$	$\dot{w} = v_i - v_r$	$\dfrac{p_i + p_r}{m} = \ddot{w} + \mu^2 w$
Single degree of freedom water backed	$\dfrac{p_k}{\rho_w c}$	$\dot{w} = v_i - v_r = v_t$	$\dfrac{p_i + p_r - p_t}{m} = \ddot{w} + \mu^2 w$
Plate bending water backed	$\dfrac{p_k}{\rho_w c}$	$\dot{w} = v_i - v_r = v_t$	$\dfrac{p_i + p_r - p_t}{m} = \ddot{w} + b^2 \nabla^4 w$
Plate bending with total energy water backed	$\dfrac{p_k}{\rho_w c} + \dfrac{1}{\rho_w R} \int_0^t p_k \, dt$	$\dot{w} = v_i - v_r = v_t$	$\dfrac{p_i + p_r - p_t}{m} = \ddot{w} + b^2 \nabla^4 w$

p_i, incident pressure; p_r, reflected pressure; p_t, transmitted pressure; w, plate deflection; m, plate's areal mass density; ρ_w, water's volumetric density; c, water's sound speed; μ, plate's in-air frequency; b, plate stiffness parameter.

5.1.2. Shock-to-structure interaction models

The study of FSIs of large plates and nearby dynamic pressure pulses has been widely studied using Taylor's model (Taylor 1963). However, Taylor's model cannot accommodate various pressure pulse shapes since it was specifically designed for a planar exponential pressure pulse. During near-field UNDEX problems, non-planar wave shapes need to be considered. Taylor's model was also designed for air-backed structures; hence, it did not account for transmitted pressures. It is critical to include transmitted pressures to broaden the applicability of an FSI model in the underwater environment. Recently, Taylor's model was validated in cases without transmitted pressures through air-backed shock loading scenarios (Sneddon 1946). Then, Taylor's model was further modified by including transmitted pressures, representing water-backed structure interactions (Sneddon 1946). A further change to Taylor's model came with integrating the plate-bending dynamics into the solution framework. This was achieved by incorporating Sneddon's (Kishore *et al.* 2020) solution for plate response to pressure loads, allowing the model to simulate structural responses beyond a single degree of freedom mass. Kishore *et al.*'s work (Sneddon 1946) also introduced near-field pressure pulse effects through the after flow fluid velocity formulation originally proposed by Arons & Yennie (1948). This addition has enabled the model to provide a more comprehensive understanding of the interaction between structures and dynamic pressures, leading to improved predictions of pressures and displacements compared with earlier models, although still limited to infinitely large elastic plates (Sneddon 1946).

These progressive enhancements in modelling FSI are outlined in table 1, showcasing the continual evolution in understanding and predicting the complex dynamics of FSI. The key limitation of these models is that they do not account for boundary conditions, cavitation effects or any phase changes in the fluid, which are often present during UNDEX. Hence, these models apply to large structures for modelling the shock–structure interactions for events where the medium does not change throughout the interaction, such as during far-field explosions or similar events.

5.1.3. Analytical solutions

The solution step involves first finding the reflected pressure and then, subsequently, all other quantities (Kishore *et al.* 2020). Upon applying the equation of continuity across the incident side and the transmitted pressure side of the plate, the governing solution of the model by Kishore *et al.* 2020 is obtained as follows:

$$p_i(t) - p_r(t) + \frac{c}{R} \int_0^t (p_i(\tau) - p_r(\tau)) \, d\tau = \lambda \int_0^t \dot{p}_r(\tau) \Omega(t - \tau) \, d\tau, \tag{5.1}$$

$$\Omega(y) = 1 - \frac{2}{\pi} \tan^{-1}\left(\frac{k}{y}\right), \tag{5.2}$$

$$\lambda = \frac{\pi s^2 \rho_w c}{8\rho h b}. \tag{5.3}$$

Where, as described in table 1, ρ_w is the density of water, c is the speed of sound in water, $p_i(t)$ is the incident pressure, $p_r(t)$ is the reflected pressure (at the plate's centre), R is the standoff distance, ρ is the density of the plate, $2h$ is the total plate thickness, s is the radial decay constant of the Gaussian pressure distribution on the plate and k is a combination of parameters that equates to $s^2/4b$. Furthermore, the plate stiffness parameter, b, can be calculated form the flexural rigidity of the plate, D, using the following (5.4) and (5.5). Lastly, λ represents a FSI parameter that combines the impedance ratio of water to the thin plate and is proportional to the circular area where the bulk of the pressure acts:

$$b^2 = \frac{D}{2\rho h}, \tag{5.4}$$

$$D = \frac{2Eh^3}{3(1 - v^2)}. \tag{5.5}$$

5.1.4. *Future analytical modelling*

Future FSI modelling efforts should focus on a more nuanced understanding of wavefronts and structural interactions. This includes addressing the complexity of the wavefront shapes and their effects on structural response, the impact of structural boundaries in this response and the inclusion of more complex material models. Further work is needed to refine models to accurately capture after flow velocities and their impact on plate deflections and transmitted pressures. This will enhance the fidelity of models in predicting the intricate interactions in underwater environments.

5.2. *Computational modelling*

5.2.1. *Computational background*

With advancing computational resources, including both hardware and sophisticated software codes, simulations of UNDEX and the resulting load on submerged structures have become a potent and cost-effective means for predictive modelling. Various theoretical formulations have been incorporated into both commercial and government-developed codes since the early 1960s (Noh 1964). This period marks when computational resources first became capable of handling such complex simulations, although the underlying theories of these codes date back even further.

These codes can be broadly categorized into two hydrocode types: Eulerian and Lagrangian. The fundamental distinction lies in the treatment of materials: in Eulerian hydrocodes, materials flow through a static grid of cells, whereas in Lagrangian hydrocodes, the mesh deforms in response to the load. For both types, energy conservation within the system is a key focus. Additionally, some codes feature a coupling interface that enables fully integrated FSI simulations. This discussion is intended to offer a concise overview of several widely used hydrocode formulations and explore how these methods are applied in simulating UNDEX and their effects on submerged structures.

5.2.2. *Eulerian fluid solver overview*

Eulerian-based computational hydrocodes are commonly utilized for simulating multi-fluid, inviscid flows, with applications spanning air/underwater shocks, laminar/turbulent flows, weather forecasting and complex fluid mixing. These Eulerian hydrocodes adeptly handle the challenges posed by significant distortions, twisting and volume loss in Lagrangian elements due to extensive deformations and severe loading. A fixed grid with regularly shaped cells is employed in Eulerian formulations, through which the various fluids navigate. This approach involves discretizing the fluid domain into a volume of regularly shaped cells that form the computational grid. Such a set-up enables the fluid to move through the grid

while the grid cells remain static, allowing fluid characteristics like velocity, density and pressure to be tracked within the cells.

The fluid's motion through these cells is dictated by fluid dynamics' conservation laws and equations, including the Euler and Navier–Stokes equations. These laws facilitate the simulation of fluid movement resulting from pressure differences and external forces, such as gravity, across discrete time steps. Mass, momentum and energy transfer calculations are performed at the junctions between cells to ensure conservation. The flow dynamics within the discretized fluid domain is determined by boundary conditions, which can be rigid boundaries (like walls and symmetry conditions) or flow boundaries (such as open faces for inflow or outflow). Eulerian solvers are recognized for their efficient scalability during parallel processing, adaptability for various transient and high-speed flow scenarios and different time scales. However, achieving high resolution in complex models often necessitates very fine meshes, leading to large model sizes and considerable demands on computational resources. Stability issues may also arise if the time-stepping methodology and size are not cautiously selected.

The origins of Eulerian-based fluid solvers date back to the 1960s, with Noh's pioneering Eulerian–Lagrangian formulation, which provided one of the initial time-dependent approaches for numerical simulations of a Lagrangian body moving through an Eulerian fluid domain. Subsequent computational developments have been made at various institutions, including the Department of Energy's creation of the KRAKEN code in the 1970s (DeBar 1974), refined later for explosives and armour strength simulations (Holian *et al.* 1989). A thorough review of hydrocodes up to the 1990s can be found in the work (Benson 1990). More recently, these codes have expanded to include applications in space and astrophysics modelling, as detailed by Trac in (Trac & Pen 2003).

5.2.3. *Coupled fluid–structure interaction methods*

In many structural applications, understanding how a structure within a fluid domain interacts with the fluid forces it encounters is crucial for predicting the structure's response. Computational methods known as FSI solvers have been developed to meet these simulation needs. Fluid–structure interaction simulations are typically employed to resolve issues where fluid flow impacts a structure, exerting forces upon it, and in turn, the structure applies forces back into the fluid. An example includes the detonation of an explosive charge near a submerged structure, where the blast pressure loads the structure, and conversely, the structure influences the shockwave.

These numerical methods utilize coupled Eulerian–Lagrangian (CEL) and arbitrary Lagrangian–Eulerian (ALE) approaches. Fluid–structure interaction coupling treats the structure and fluid as separate entities linked by a coupling interface. The fluid is modelled using the Eulerian method in the simulations, while the structure is modelled using the Lagrangian approach. They operate independently and exchange crucial variables after each integration step. The structure's surface within the fluid is delineated by a stair-step boundary technique, and interface elements that are either singly or doubly wetted define the contact with the fluid. This method is elaborated with benchmark examples in Wardlaw *et al.* (2004). The ALE method models the structure with Lagrangian mesh coordinates that interact with the fluid, while the fluid mesh is Eulerian. Periodic re-meshing reconciles these domains into a single reference frame. Detailed descriptions of ALE formulations can be found in Le Tallec & Mouro (2000), Souli *et al.* (2000), Legay *et al.* (2006) and Noble *et al.* (2017).

A common challenge with CEL and ALE methods is the appearance of non-physical spurious oscillations near the material interfaces within the fluid. These artifacts arise from issues like material density smearing and abrupt changes in the Equation of state at the interface (e.g., water-to-air transition). To tackle these issues, a novel approach known as the ghost fluid method was introduced in the late 1990s by Fedkiw *et al.* (1999). This level-set method for multiphase flows achieves sharp delineation at surface discontinuities by using a layer of ghost cells to maintain continuous pressure and velocity profiles at the discontinuity. The ghost method has been refined to enhance its precision and adaptability. Wang *et al.* (2008) developed an adaptive ghost method, blending the ghost fluid method with adaptive meshing to harness the strengths of both. Specifically for simulating underwater implosions, Farhat has further refined the ghost method into the ghost fluid method for the poor (Farhat *et al.* 2008). This

method leverages arbitrary equations of state with advanced multi-step time integration techniques, proving effective in handling large density and pressure discontinuities at interfaces.

5.2.4. *Underwater explosion simulations*

The methods previously discussed model full fluid domains numerically and computationally. Depending on the mesh size and resolution, these methods can lead to sizable models that require substantial computational resources to achieve accurate results. In contrast, analytical modelling methods for predicting structural responses to dynamic shock loading provide more time-efficient solutions for UNDEX scenarios, although they come with their own limitations. Geers introduced the doubly asymptotic approximation (DAA) for transient analysis of structures within a fluid (Geers 1978), using differential equations to approximate the behaviour of wetted surfaces under dynamic pressure conditions. This method obviates the need for discretizing the fluid domain, substantially reducing computational costs. The original implementation was later used to study the steady-state vibration of submerged structures (Geers & Felippa 1983). The DAA method underpins the underwater shock analysis code (DeRuntz *et al.* 1978) for modelling spherical shock impacts on structures. For modelling surface ship responses to UNDEX, Shin (2004) used a finite element method for the ship and near-field fluid coupled with the DAA approach to minimize the fluid domain. Lastly, Riley (2010) summarized nine unique analytical techniques for predicting the behaviour of underwater gas bubbles from explosions, correlating models for bubble radius over time.

5.2.5. *Explosion and bubble dynamics simulations*

5.2.5.1. *Free field*

Simulating underwater explosive detonations is inherently a highly nonlinear and complex computational challenge. The explosion of submerged charges creates sharply curved, transient pressure profiles characterized by narrow wavefronts and high velocities. Moreover, the resultant bubble – a complex mix of gaseous combustion products – undergoes expansion and collapse, forming an intricate interface with the surrounding fluid. Additional complexity arises when simulating the bubble pulses that occur at later stages, requiring the simulation to maintain numerical stability to accurately depict the long-term behaviour of the bubble and pressure pulses. Refining fluid cells is critical to capture these narrow shock fronts emanating from the detonation point, which must be balanced against computational resources to avoid averaging or smearing the shock pressures while maintaining manageability.

A substantial body of literature exists on computational methods for simulating free-field detonations of explosive charges. Liu *et al.* (2018*b*) applied the Eulerian method to simulate a free-field detonation at varying depths, initially outlining the theoretical formulation and then demonstrating the method for early pressure wave and later bubble oscillation simulations. They analysed the differential pressure effects above and below the bubble. This work was extended in subsequent research, where the authors developed an Abaqus subroutine to continuously simulate UNDEX physics, validating the subroutine's accuracy through simulations of detonation, bubble dynamics and jetting behaviours (Liu *et al.* 2018*a*). A two-phase formulation for UNDEX simulation using finite volume differencing and correlations to experimental data for free-field detonations and interactions with rigid bodies were presented in Nguyen *et al.* (2021). Another combined method, integrating the finite volume approach with the volume of fluid techniques for modelling underwater explosion bubble dynamics, was discussed in Li *et al.* (2018), including validation against spherical bubbles and buoyancy-affected bubbles.

Shende introduced an innovative iso-geometric formulation and level-set approach for UNDEX modelling in Shende & Bazilevs (in press), validated against experimental data of various complexities. Wu *et al.* (2020) presented a model capturing the influence of the fluid's free surface on bubble dynamics and surface cavitation. An overarching consideration in these sophisticated UNDEX analyses is achieving the right mesh resolution balance – precise enough for an accurate solution yet economical regarding computational resources and time. A method to determine appropriate mesh sizes for different UNDEX

scenarios, based on developing a non-dimensional variable correlating the charge radius to element size, has been evaluated in (Wang *et al.* 2016) and shown to be effective for a range of charge sizes.

5.2.5.2. *Near field to adjacent plates and structures*

When evaluating the effects of an underwater explosion on nearby structures, it is crucial to incorporate these structures into the FSI model and accurately represent the detonation process. The interaction between the detonation pressure wave and the structure is often intense, especially for near-field detonations. The structure's geometry and stiffness can influence the pressure front and its reflection toward the bubble's centre. Javier *et al.* (2020a) investigated how the standoff distance of a charge from a rigid steel plate impacts the bubble's interaction with the structure. Their research showed that the standoff distance significantly affects bubble characteristics, including its shape, the pressure on the structure and bubble migration and jetting during the growth and collapse phases, as illustrated in figure 3.

A discussion on the impact of UNDEX on thin metallic structures, considering FSI effects such as bubble pulsation and cavitation, is provided in Nagesh & Gupta (2021). Further research on the effects of UNDEX on metallic plates is found in Gupta *et al.* (2010), examining the failure of high-strength steel plates due to an exponentially decaying UNDEX pressure front, including the spatial and temporal variations.

The UNDEX response of submerged cylindrical structures has also been studied, presenting additional complexities in structural loading due to the curved nature of the incident wavefront and the structure itself. Wang *et al.* (2020) analysed the response of a vertical cylinder to underwater shock, breaking down the total pressure into incident, scattered and radiated components to understand the cylinder's dynamic response. Gannon (2019) numerically studied the response of a stiffened submerged cylinder, focusing on the effects of the shock and bubble jet, with results measured by bubble dynamics and structural strain and displacement. Yapar & Basu (2022) introduced a novel approach using the Abaqus explicit solver coupled with the XFlow computational fluid dynamics solver to simulate the nonlinear response of submerged structures to shock waves, validated with test data for a submerged tubular structure under UNDEX pressure waves.

Incorporating lightweight composite materials in marine structures makes understanding their response to UNDEX loading increasingly important. Tran *et al.* (2021) reviewed key studies on composite materials subjected to UNDEX, including experimental and numerical analyses. Achor *et al.* (2022) investigated the failure of carbon fibre laminates under UNDEX conditions, comparing experimental results with computational simulations. Dyka & Badaliance (1998) created damage models for predicting the shock response of thick marine composite plates.

Recent attention has focused on the collapse of submerged cylindrical bodies due to nearby UNDEX. Ma *et al.* (2022) proposed a multiphase FSI procedure to analyse the collapse of a thin-walled aluminium cylinder triggered by a close-range detonation, noting that the cylinder's collapse also affects the gas bubble dynamics. Numerical modelling and theoretical analysis of the dynamic stability of submerged thin-walled cylinders subjected to UNDEX were conducted in Sun *et al.* (2022), explicitly employing an acoustic element formulation in Abaqus to simulate the water domain. The study identified a hydrostatic pre-pressure threshold above which the cylinders would collapse from the shock-induced vibrations. Guzas *et al.* (2019) used the CEL solver DYSMAS to evaluate the dynamic stability of a cylindrical shell under combined hydrostatic and dynamic loading, accurately predicting the threshold for failure onset when combining hydrostatic pre-pressure with UNDEX shock loading.

5.2.6. *Limitations*

A key limitation of computational modelling is the computational expanse of high-reliability models. This expanse is extreme for underwater explosion simulations when the underwater bubble effects, such as near-field explosion events, must be considered. This is because of the difference in time scales: the shock interaction event happens on the microsecond scale, the first bubble interaction will happen within tens of milliseconds, and the entire bubble–structure interaction may be in the hundreds of milliseconds scale. The event may be on the second or higher scale for larger explosives. It is widely understood

that total simulation time is highly influenced, if not dominated, by the smallest time events. Hence, multiple events in different time scales will not be computationally time-efficient. Recent computation modelling of such events for simple rigid structures and small charge sizes (Javier *et al.* 2020*a*) took tens of thousands of CPU hours to simulate up to the first bubble interaction. A high-reliability model for an entire near-field explosion event that includes bubble oscillation behaviour would be a massive undertaking, and it is not a feasible modelling solution.

Other limitations of explosion computational modelling are challenges with the fluid and solid solvers. For fluids, most commercial solvers do not handle fluid phase change (such as cavitation effects) well, if at all. This is a huge limitation for near-field explosions, but there is much ongoing work trying to address such limitations with fluid solvers (Tian *et al.* 2021; Yu *et al.* 2022, 2023*a*; Yu, Song & Choi 2023*b*). Modelling the dynamic and failure behaviour of complex materials such as composites is also challenging for solids. Recent work has addressed some of these challenges by including the interplay behaviour of composites in the modelling (Ulbricht *et al.* 2024). Material models, such as LS-DYNA's MAT213, have been developed to capture the dynamic viscoelastic-temperature behaviour of anisotropic materials. Nonetheless, to develop these more accurate modelling approaches and material models, a huge undertaking for testing and characterizing the unique behaviour specific to each composite system is often required to validate modelling parameters. This review does not discuss all these intricacies and novelties with computational simulations. These topics warrant additional considerations and their dedicated review when developing computation models.

6. Concluding remarks

The comprehensive review of UNDEX underscore the intricate and multifaceted nature of these phenomena. This study highlights the critical need for advanced research and development in understanding and mitigating the effects of UNDEX. It is established that the relatively incompressible nature of water plays a significant role in the behaviour of shock waves and gas bubbles, which are critical components of UNDEX. These insights are vital for designing more resilient maritime structures and vessels capable of withstanding the intense forces generated by UNDEX. Future research should continue to focus on innovative solutions and technologies to enhance the protection of maritime assets against these complex underwater threats.

References

Achor, C.H., Kwon, Y.W., Didoszak, J.M., Crow, N.E. and Hardman, D.J. 2022 Study of air-backed and water-backed carbon fiber composite plates subjected to underwater shock loading. *Compos. Struct.* **300**, 116147.

Arons, A.B. 1948 Secondary pressure pulses due to gas globe oscillation in underwater explosions. II. Selection of adiabatic parameters in the theory of oscillation. *J. Acoust. Soc. Am.* **20** (3), 277–282.

ARONS, A.B., SLIFKO, J.P. & CARTER, A. 1948 Secondary pressure pulses due to gas globe oscillation in underwater explosions. I. Experimental data. *J. Acoust. Soc. Am.* **20** (3), 271–276.

ARONS, A.B. & YENNIE, D.R. 1948 Energy partition in underwater explosion phenomena. *Rev. Mod. Phys.* **20**, 3.

BENJAMIN, T.B. & ELLIS, A.T. 1966 The collapse of cavitation bubbles and the pressures thereby produced against solid boundaries. *Phil. Trans. R. Soc. Lond.* **260**, 221–240.

BENSON, D.J. 1990 Computational methods in Lagrangian and Eulerian hydrocodes. University of California San Diego.

BLAKE, J.R. & GIBSON, D.C. 1987 Cavitation bubbles near boundaries. *Annu. Rev. Fluid Mech.* **19** (1), 99–123.

BRUJAN, E.-A., NAHEN, K., SCHMIDT, P. & VOGEL, A. 2001 Dynamics of laser-induced cavitation bubbles near elastic boundaries: influence of elastic modulus. *J. Fluid Mech.* **433**, 283–314.

CHAPMAN, R.N. 1985 Measurements of the waveform parameters of shallow explosive charges. *J. Acoust. Soc. Am.* **78**, 2.

CHAUDHARY, B., LI, H. & MATOS, H. 2023 Long-term mechanical performance of 3D printed thermoplastics in seawater environments. *Results Mater.* **17**, 100381.

CHAUDHARY, B., LI, H., NGWA, A.N. & MATOS, H. 2024 Investigating the effects of coating systems on the degradation behavior of 3D-printed pressure vessels. *Mar. Struct.* **93**, 103540.

CHEN, S., XU, H., DUAN, H., HUA, M., WEI, L., SHANG, H. & LI, J. 2017 Influence of hydrostatic pressure on water absorption of polyoxymethylene: experiment and molecular dynamics simulation. *Polym. Adv. Technol.* **28** (1), 59–65.

CHENWI, I.N., RAMOTOWSKI, T., LEBLANC, J. & SHUKLA, A. 2022 Effects of prolonged saline water exposure on the peel strength of polyurea/monel 400 interface. *J. Adhes.* **98** (10), 1377–1393.

CHERTOCK, G. 1953 The flexural response of a submerged solid to a pulsating gas bubble. *J. Appl. Phys.* **24**, 192–197.

COLE, R.H. 1948 *Underwater Explosions*. Princeton University Press.

DAI, L.H., WU, C., AN, F.J. & LIAO, S.S. 2018 Experimental investigation of polyurea-coated steel plates at underwater explosive loading. *Adv. Mater. Sci. Engng* **2018**, 1–7.

DAVIES, P. 2016 Environmental degradation of composites for marine structures: new materials and new applications. *Phil. Trans. R. Soc.* A*: Math. Phys. Engng Sci.* **374** (2071), 20150272.

DEBAR, R. 1974 *Fundamentals of the KRAKEN Code*. Lawrence Livermore Laboratory.

DERUNTZ, J., GEERS, T. & FELIPPA, C. 1978 The underwater shock analysis (USA) code – a reference manual. *Tech. Rep.* DNA 4524F. Defense Nuclear Agency.

DESHPANDE, V.S. & FLECK, N.A. 2005 One-dimensional response of sandwich plates to underwater shock loading. *J. Mech. Phys. Solids* **53**, 2347–2383.

DUNCAN, J.H., MILLIGAN, C.D. & ZHANG, S. 1996 On the interaction between a bubble and submerged compliant structure. *J. Sound Vib.* **197**, 17–44.

DYKA, C.T. & BADALIANCE, R. 1998 Damage in marine composites caused by shock loading. *Compos. Sci. Technol.* **58** (9), 1433–1442.

ESPINOSA, H.D., LEE, S. & MOLDOVAN, N. 2006 A novel fluid structure interaction experiment to investigate deformation of structural elements subjected to impulsive loading. *Exp. Mech* **46**, 805–824.

EZRA, A.A. 1973. *Principles and Practice of Explosive Metalworking*, vol. 1. Industrial Newspapers.

FARHAT, C., RALLU, A. & SHANKARAN, S. 2008 A higher-order generalized ghost fluid method for the poor for the three-dimensional two-phase flow computation of underwater implosions. *J. Comput. Phys.* **227** (16), 7674–7700.

FEDKIW, R., ASLAM, T., MERRIMAN, B. & OSHER, S. 1999 A non-oscillatory Eulerian approach to interfaces in multimaterial flows (the ghost fluid method). *J. Comput. Phys.* **152**, 457–492.

FONTAINE, D., LEBLANC, J. & SHUKLA, A. 2021 Blast response of carbon-fiber/epoxy laminates subjected to long-term seawater exposure at sea floor depth pressures. *Compos.* B*: Engng* **215**, 108647.

FRIEDLANDER, F.G. 1941 *The pressure and impulse of submarine explosion waves on plates*. Civil Defense Research Committee, Ministry of Home Security.

GALIEV, S.U. 1979 *Numerical investigation of the deformation of plates by liquid in press gun*. Institute of Strength Problems.

GALIEV, S.U. 1987 *Unexpected behaviour of plates during shock and hydrodynamic loading*. Institute of Strength Problems.

GALIEV, S.U. 1995 Experimental observations and discussion of counterintuitive behavior of plates and shallow shells subjected to blast loading. *Intl J. Impact Engng* **18**, 783–802.

GALIEV, S.U. 1997 Influence of cavitation upon anomalous behaviour of a plate/liquid/underwater explosion system. *Intl J Impact Engng* **19**, 345–359.

GANNON, L. 2019 Submerged aluminum cylinder response to close-proximity underwater explosions – a comparison of experiment and simulation. *Intl J Impact Engng* **133**, 103339.

GAUCH, E., LEBLANC, J. & SHUKLA, A. 2018 Near field underwater explosion response of polyurea coated composite cylinders. *Compos. Struct.* **202**, 836–852.

GEERS, T. 1978 Doubly asymptotic approximations for transient motions of submerged structures. *J. Acoust. Soc. Am.* **64**, 1500–1508.

GEERS, T. & FELIPPA, C. 1983 Doubly asymptotic approximations for vibration analysis of submerged structures. *J. Acoust. Soc. Am.* **73**, 1152–1159.

GIBSON, D.C. 1968 Cavitation adjacent to plane boundaries. In *Proceedings of the Conference on Hydraulics and Fluid Mechanics, Sydney*, pp. 210–214.

GIBSON, D.C. & BLAKE, J.R. 1982 The growth and collapse of bubbles near deformable surfaces. *Appl. Sci. Res.* **38**, 215–224.

GUPTA, N.K., KUMAR, P. & HEGDE, S. 2010 On deformation and tearing of stiffened and un-stiffened square plates subjected to underwater explosion—a numerical study. *Intl J. Mech. Sci.* **52**, 733–744.

GUZAS, E., GUPTA, S., AMBRICO, J., LEBLANC, J. & SHUKLA, A. 2019 Computational modeling of dynamically initiated instabilities and implosion of underwater cylindrical structures in a confined environment. *J. Appl. Mech.* **86** (2), 021008.

HE, H. & FAN, H. 2021 Explosion vibration mitigation of meta-plate with mass–spring metastructures. *Extreme Mech. Lett.* **42**, 101108.

HUMEAU, C. & DAVIES, P. 2015 Moisture diffusion under hydrostatic pressure in composites. *Mater. Des.* **96**, 19.

HUNG, C.F., HSU, P.Y. & HWANG-FUU, J.J. 2005 Elastic shock response of an air-backed plate to underwater explosion. *Intl J. Impact Engng* **31**, 151–168.

JAVIER, C., GALUSKA, M., PAPA, M., LEBLANC, J., MATOS, H. & SHUKLA, A. 2020*a* Underwater explosive bubble *interaction with an adjacent submerged structure*. *J. Fluids Struct.* **100**, 103189.

JAVIER, C., LEBLANC, J. & SHUKLA, A. 2020*b* Hydrothermally degraded carbon fiber/epoxy plates subjected to underwater explosive loading in a fully submerged environment. *Mar. Struct.* **72**, 102761.

JAVIER, C., MATOS, H. & SHUKLA, A. 2018 Hydrostatic and blast initiated implosion of environmentally degraded Carbon-Epoxy composite cylinders. *Compos. Struct.* **202**, 897–908.

JAVIER, C., SMITH, T., LEBLANC, J. & SHUKLA, A. 2019 Effect of prolonged ultraviolet radiation exposure on the blast response of fiber reinforced composite plates. *J. Mater. Engng Perform.* **28** (6), 3174–3185.

JUNGER, M.C. & FEIT, D. 1986 *Sound, Structures, and their Interaction*. MIT Press.

KEIL, A.A.H. 1961 The response of ships to underwater explosions. *Trans. Soc. Nav. Archit. Mar. Engng* **69**, 366–410.

KENNARD, E.H. 1944 *The Effect of a Pressure Wave on a Plate or Diaphragm*. David Taylor Model Basin.

KIM, Y.-H. 2010 *Sound Propagation: An Impedance Based Approach*. John Wiley & Sons.

KISHORE, S., SENOL, K., PARRIKAR, P.N. & SHUKLA, A. 2020 Underwater implosion pressure pulse interactions with submerged plates. *J. Mech. Phys. Solids*. https://doi.org/10.1016/j.jmps.2020.104051

KONFELD, M. & SUVOROV, L. 1944 On the destructive action of cavitation. *J. Appl. Phys.* **15**, 495–506.

KUMAR, B.G., SINGH, R.P. & NAKAMURA, T. 2002 Degradation of carbon fiber-reinforced epoxy composites by ultraviolet radiation and condensation. *J. Compos. Mater.* **36** (24), 2713–2733.

KWON, Y.W., BERGERSEN, J.K. & SHIN, Y.S. 1994 Effect of surface coatings on cylinders exposed to underwater shock. *Shock Vib.* **1** (3), 253–265.

LAUTERBORN, W. & BOLLE, H. 1975 Experimental investigations of the cavitation-bubble collapse in the neighbourhood of a solid boundary. *J. Fluid Mech.* **72** (2), 391–399.

LE TALLEC, P. & MOURO, J. 2000 Fluid structure interaction with large structural displacements. *Comput. Meth. Appl. Mech. Engng* **190**, 3039–3067.

LEBLANC, J., GARDNER, N. & SHUKLA, A. 2013 Effect of polyurea coatings on the response of curved E-Glass/Vinyl ester composite panels to underwater explosive loading. *Compos. B: Engng* **44** (1), 565–574.

LEBLANC, J. & SHUKLA, A. 2015 Response of polyurea-coated flat composite plates to underwater explosive loading. *J. Compos. Mater.* **49** (8), 965–980.

LEBLANC, J., SHILLINGS, C., GAUCH, E., LIVOLSI, F. & SHUKLA, A. 2016 Near field underwater explosion response of polyurea coated composite plates. *Exp. Mech.* **56** (4), 569–581.

LEGAY, A., CHESSA, J. & BELYTSCHKO, T. 2006 An Eulerian-Lagrangian method for fluid-structure interaction based on level sets. *Comput. Meth. Appl. Mech. Engng* **195**, 2070–2087.

LEGER, M., MATOS, H., SHUKLA, A. & JAVIER, C. 2023 Experimental evaluation of curved aluminum structures subjected to underwater explosions. *Exp. Mech.* **63** (5), 925–937.

LI, T., WANG, S. & ZHANG, A. 2018 Numerical investigation of an underwater explosion bubble based on FVM and VOF. *Appl. Ocean Res.* **74**, 49–58.

LI, Y., CHEN, Z., ZHAO, T., CAO, X., JIANG, Y., XIAO, D. & FANG, D. 2019 An experimental study on dynamic response of polyurea coated metal plates under intense underwater impulsive loading. *Intl J. Impact Engng* **133**, 103361.

LIU, J., AN, F., NIU, Z., ZHANG, L., FENG, B., LI, Y. & WU, C. 2022*a* Study on the blast-resistance of polyurea-steel plates subjected to underwater explosion. *Ocean Engng* **265**, 111814.

LIU, J., AN, F.-J., WU, C., LIAO, S.S., ZHOU, M.-X., XUE, D.-Y. & GUO, H. 2022*b* Experimental investigations on small-and full-scale ship models with polyurea coatings subjected to underwater explosion. *Def. Technol.* **18** (7), 1257–1268.

LIU, W., MING, F., ZHANG, A., MIAO, X. & LIU, Y. 2018*a* Continuous simulation of the whole process of underwater explosion based on Eulerian finite element approach. *Appl. Ocean Res.* **80**, 125–135.

LIU, Y., ZHANG, A., TIAN, Z. & WANG, S. 2018*b* Investigation of free-field underwater explosion with Eulerian finite element method. *Ocean Engng* **166**, 182–190.

LIU, Z. & YOUNG, Y.L. 2008 Transient response of submerged plates subject to underwater shock loading: an analytical perspective. *J. Appl. Mech.* **75**, 044504.

MA, W., ZHAO, X., GILBERT, C. & WANG, K. 2022 Computational analysis of bubble–structure interactions in nearfield underwater explosion. *Intl J. Solids Struct.* **242**, 111527.

MANDELL, D.A., ADAMS, T.F., HOLIAN, K.S., ADDESSIO, F.L., BAUMGARDNER, J.R. & MOSSO, S.J. 1989 MESA: A 3-D computer code for armor/anti-armor applications. *Tech. Rep.* LA-UR-89-1851; CONF-8910103-1. Los Alamos National Laboratory.

Matos, H., Javier, C., LeBlanc, J. & Shukla, A. 2018 Underwater nearfield blast performance of hydrothermally degraded carbon–epoxy composite structures. *Multiscale Multidiscip. Model. Exp. Des*. **1** (1), 33–47.

McMeeking, R.M., Spuskanyuk, A.V., He, M.Y., Deshpande, V.S., Fleck, N.A. & Evans, A.G. 2008 An analytic model for the response to water blast of unsupported metallic sandwich panels. *Intl J. Solids Struct* **45**, 478–496.

Mohotti, D., Fernando, P.L.N., Weerasinghe, D. & Remennikov, A. 2021 Evaluation of effectiveness of polymer coatings in reducing blast-induced deformation of steel plates. *Def. Technol*. **17** (6), 1895–1904.

Nagesh & Gupta, N.K. 2021 Response of thin-walled metallic structures to the underwater explosion: a review. *Intl J. Impact Engng* **156**, 103950.

Naudé, C.F. & Ellis, A.T. 1960 *On the mechanism of cavitation damage by non-hemispherical cavities in contact with a solid boundary*. Department of the Navy.

Nayak, S., Lyngdoh, G.A., Shukla, A. & Das, S. 2022 Predicting the near field underwater explosion response of coated composite cylinders using multiscale simulations, experiments, and machine learning. *Compos. Struct*. **283**, 115157.

Neba Mforsoh, I., LeBlanc, J. & Shukla, A. 2020 Constitutive compressive behavior of polyurea with exposure to aggressive marine environments. *Polymer Test*. **85**, 106450.

Nguyen, V., Phan, T., Duy, T. & Park, W. 2021 Numerical modeling for compressible two-phase flows and application to nearfield underwater explosions. *Comput. Fluids* **215**, 104805.

Noble, C., *et al.* 2017 ALE3D: an arbitrary Lagrangian-Eulerian multi-physics code. *Tech. Rep.* LLNL-TR-732040. Lawrence Livermore National Laboratory.

Noh, W.F. 1964 *CEL: A Time-Dependent, Two Space Dimensional, Coupled Eulerian-LaGrange Code*. University of California Lawrence Radiation Laboratory.

Pavlov, A.A. & Galiev, S.U. 1977 *Experimental investigation of the cavitation interaction of a compression wave with a plate in liquid*. Institute of Strength Problems.

Plesset, M.S. & Chapman, R.B. 1970 Collapse of an initially spherical vapour cavity in the neighbourhood of a solid boundary. *J. Fluid Mech*. **47**, 283–290.

Pollard, A., Baggott, R., Wostenholm, G.H., Yates, B. & George, A.P. 1989 Influence of hydrostatic pressure on the moisture absorption of glass fibre-reinforced polyester. *J. Mater. Sci*. **24** (5), 1665–1669.

Rajendran, R., Paik, J.K. & Kim, B.J. 2006 Design of warship plates against underwater explosions. *Ships Offshore Struct*. **1**, 347–356.

Ramajeyathilagam, K. & Vendham, C.P. 2003 Underwater explosion of ship hull panels. *Def. Sci. J*. **53**, 393–402.

Ramajeyathilagam, K. & Vendham, C.P. 2004 Deformation and rupture of thin rectangular plates subjected to underwater shock. *Intl J. Impact Engng* **30**, 699–719.

Ramajeyathilagam, K., Vendhan, C.P. & Rao, B.V. 2000 Nonlinear transient dynamic response of rectangular plates under shock loading. *Intl J. Impact Engng*. **24** (10), 999–1015.

Ramajeyathilagam, K., Vendham, C.P. & Rao, B.V. 2001 Experimental and numerical investigations on deformation of cylindrical shell panels to underwater explosion. *Shock Vib*. **8**, 253–270.

Ramamurthi, K. 2021 *Modeling Explosions and Blast Waves*. Springer.

Rayleigh, L. 1917 On the pressure developed in a liquid during the collapse of a spherical void. *Phil. Mag*. **34**, 94–98.

Rice, M. and Ramotowski, T. 2011 Activation energy calculation for the diffusion of water into PR-1590 and pellethane 2103-80AW polyurethanes. *Tech. Memo* 11-062. NUWC-NPT.

Riley, M. 2010 Analytical solutions for predicting underwater explosion gas bubble behaviour, DRDC Atlantic TM 2010-23.

Riley, M.J., Paulgaard, G.T., Lee, J.J. & Smith, M.J. 2010 Failure mode transition in air-backed plates from near contact underwater explosions. *Shock Vib*. **17**, 723–739.

Roland, C.M., Twigg, J.N., Vu, Y. & Mott, P.H. 2007 High strain rate mechanical behavior of polyurea. *Polymer* **48** (2), 574–578.

Shende, S. & Bazilevs, Y. in press A new stabilized formulation for the simulation of underwater explosions using isogeometric analysis. *Comput. Meth. Appl. Mech. Engng*.

Shillings, C., Javier, C., LeBlanc, J., Tilton, C., Corvese, L. & Shukla, A. 2017 Experimental and computational investigation of the blast response of carbon-epoxy weathered composite materials. *Compos. B: Engng* **129**, 107–116.

Shima, A., Gibson, D.C. & Blake, J.R. 1988 The growth and collapse of cavitation bubbles near composite surfaces. *J. Fluid Mech*. **203**, 199–214.

Shin, Y.S. 2004 Ship shock modeling and simulation for far-field underwater explosion. *Comput. Struct*. **82**, 2211–2219.

Sneddon, I.N. 1946 The elastic response of a large plate to a Gaussian distribution of pressure varying with time. *Math. Proc. Camb. Phil. Soc*. **42**, 338–341.

Souli, M., Ouahsine, A. & Lewin, L. 2000 ALE formulation for fluid-structure interaction problems. *Comput. Meth. Appl. Mech. Engng* **190**, 659–675.

Sun, W., Zhu, T., Chen, P. & Lin, G. 2022 Dynamic implosion of the submerged cylindrical shell under the combined hydrostatic and shock loading. *Thin-Walled Struct*. **170**, 108574.

Suresh, C. & Ramajeyathilagam, K. 2020 Coupled fluid-structure interaction based numerical investigation on the large deformation behavior of thin plates subjected to under water explosion. *Intl J. Veh. Struct. Syst*. **12**, 436–442.

Suresh, C. & Ramajeyathilagam, K. 2021 Large deformation behaviour of thin mild steel rectangular plates subjected to underwater explosion loading under air and water backed conditions. *Appl. Ocean Res*. **114**, 102780.

Swisdak, M. 1978 Explosion effects and properties. Part II. Explosion effects in water. https://doi.org/10.21236/ada056694

TAYLOR, G.I. 1963 The pressure and impulse of submarine explosion waves on plates. In *The Scientific Papers of G. I. Taylor*.

TEICH, M. & GEBBEKEN, N. 2013 Analysis of FSI effects of blast loaded flexible structures. *Engng Struct*. **55**, 73–79.

TEKALUR, S.A., SHUKLA, A. & SHIVAKUMAR, K. 2008 Blast resistance of polyurea based layered composite materials. *Compos. Struct*. **84** (3), 271–281.

TEMPERLEY, H.N.V. 1950 Theoretical investigation of cavitation phenomena occurring when an underwater pressure pulse is incident on a yielding surface. Underwater Explosion Research.

TIAN, Z.L., ZHANG, A.M., LIU, Y.L. & TAO, L. 2021 A new 3-D multi-fluid model with the application in bubble dynamics using the adaptive mesh refinement. *Ocean Engng* **230**, 108989.

TRAC, H. & PEN, U. 2003 A primer of Eulerian computational fluid dynamics for astrophysics. *Astron. Soc. Pacific* **115**, 303–321.

TRAN, P., WU, C., SALEH, M., NETO, L., NGUYEN-XUAN, H. & FERREIRA, A. 2021 Composite structures subjected to underwater explosive loadings: a comprehensive review. *Compos. Struct*. **263**, 113684.

ULBRICHT, N., BOLDINI, A., ZHANG, P. & PORFIRI, M. 2024 Three-dimensional analytical solution of free vibrations of a simply supported composite plate in contact with a fluid. *J. Sound Vib*. **572**, 118139.

WANCHOO, P., CHAUDHARY, B., MATOS, H. & SHUKLA, A. 2023 Blast failure and energy analysis of rubber-modified carbon-fiber vinyl-ester composite laminates. *Mech. Mater*. **183**, 104685.

WANCHOO, P., MATOS, H., ROUSSEAU, C.E. & SHUKLA, A. 2021 Investigations on air and underwater blast mitigation in polymeric composite structures – a review. *Compos. Struct*. **263**, 113530.

WANCHOO, P., PANDEY, A., LEGER, M., LEBLANC, J. & SHUKA, A. 2024 Energy quantification framework for underwater explosive loading on PVC cladded composite plates. *J. Mech. Phys. Solids*, 105646.

WANG, C., TANG, H. & LIU, T. 2008 An adaptive ghost fluid finite volume method for compressible gas–water simulations. *J. Comput. Phys*. **227** (12), 6385–6409.

WANG, G., WANG, Y., LU, W., ZHOU, W., CHEN, M. & YAN, P. 2016 On the determination of the mesh size for numerical simulations of shock wave propagation in near field underwater explosion. *Appl. Ocean Res*. **59**, 1–9.

WANG, P., ZHANG, Z., YAN, Q. & ZHANG, C. 2020 A substructure method for the transient response of vertical cylinders subjected to shock wave of underwater explosion. *Ocean Engng* **218**, 108128.

WANG, Z., LIANG, X. & LIU, G. 2013 An analytical method for evaluating the dynamic response of plates subjected to underwater shock employing Mindlin plate theory and Laplace transforms. *Math. Probl. Engng* **2013**, 1–11.

WARDLAW, A., LUTON, J.A., RENZI, J. & KIDDY, K. 2004 Fluid-structure coupling methodology for undersea weapons. *Trans. Built Environ*. **71**, https://doi.org/10.2495/FSI030241.

WU, W., LIU, Y., ZHANGE, A., LIU, N. & LIU, L. 2020 Numerical investigation on underwater explosion cavitation characteristics near water wave. *Ocean Engng* **205**, 107321.

XUE, Z. & HUTCHINSON, J.W. 2004 A comparative study of impulse-resistant metal sandwich plates. *Intl J. Impact Engng* **30**, 1283–1305.

YAPAR, O. & BASU, P.K. 2022 Fluid-structure interaction simulation of the effects of underwater explosion on submerged structures. *Finite Elem. Anal. Des*. **199**, 103678.

YI, J., BOYCE, M.C., LEE, G.F. & BALIZER, E. 2006 Large deformation rate-dependent stress-strain behavior of polyurea and polyurethanes. *Polymer* **47** (1), 319–329.

YU, J., LIU, J.H., WANG, H.K., WANG, J., ZHOU, Z.T. & MAO, H.B. 2022 Application of two-phase transition model in underwater explosion cavitation based on compressible multiphase flows. *AIP Adv*. **12**, 2.

YU, J., WANG, H.K., SHENG, Z.X. & HAO, Y. 2023*a* Investigation on strong nonlinear interactions between underwater explosion and water surface based on compressible multiphase flow with phase transition. *J. Hydrodyn*. **35** (2), 351–364.

YU, W., SONG, S. & CHOI, J.I. 2023*b* Numerical simulations of underwater explosions using a compressible multi-fluid model. *Phys. Fluids* **35**, 10.